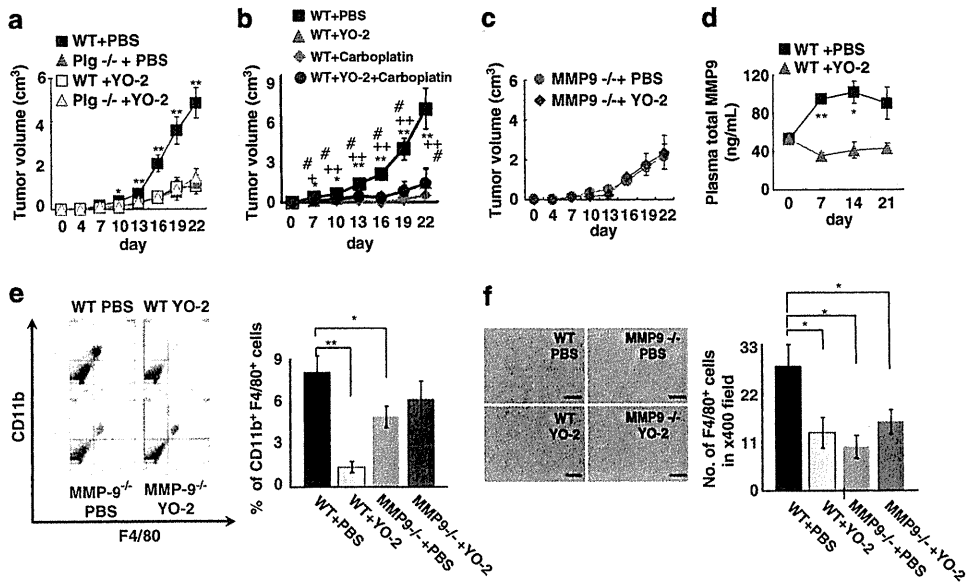

Figure 3 Plm inhibitor blocks lymphoma growth by suppressing MMP-9-dependent $CD11b^+F4/80^+$ cell recruitment. (**a–c**) $MMP\text{-}9^{-/-}$ and $Plg^{-/-}$ and corresponding WT control mice were injected subcutaneously with B6RV2 cells and treated intra-peritoneal with/without Plm inhibitor YO-2. (**a–c**) Lymphoma volume was measured at different time points after cell inoculation (**a**): $n=9$ for WT mice; $n=10$ for YO-2-treated WT mice; $n=9$ for $MMP\text{-}9^{-/-}$ mice; $n=10$ for YO-2-treated $MMP\text{-}9^{-/-}$ mice; $n=5$ for YO-2-treated $Plg^{-/-}$ mice; $^*P<0.05$ and $^{**}P<0.01$ comparing WT with YO-2-treated WT mice, (**b**, **c**); $n=4$ $^{*+\#}P<0.05$ and $^{**\ +\ +\#\#}P<0.01$). (**d**) ELISA assay for measurement of total MMP-9 levels in plasma samples obtained from WT mice treated with or without YO-2 ($n=3$; $^*P<0.05$ and $^{**}P<0.01$ comparing WT with YO-2-treated WT mice). (**e**, **f**) $MMP\text{-}9^{-/-}$ and WT mice were injected subcutaneously with B6RV2 cells and treated intra-peritoneal with/without Plm inhibitor YO-2. (**e**) On day 7, the number of $CD11b^+F4/80^+$ cells was determined by FACS within crushed lymphoma tissues of the mice ($n=11$ for WT and $n=6$ for YO-2-treated WT-derived cells; $n=11$ for $MMP\text{-}9^{-/-}$ and $n=8$ for YO-2-treated $MMP\text{-}9^{-/-}$-derived cells; $^*P<0.05$ and $^{**}P<0.01$) (**f**) The density of $F4/80^+$ cells was quantified in day 7 lymphoma tissues ($n=4$ for WT and $n=7$ for YO-2-treated WT-derived lymphoma tissue; $^*P<0.05$ and $^{**}P<0.01$, and $n=4$ for $MMP\text{-}9^{-/-}$ or $n=8$ for YO-2-treated $MMP\text{-}9^{-/-}$-derived lymphoma tissue). Scale bar = 100 μm.

(Figure 3d). These results indicate that B6RV2 lymphoma growth is controlled by Plg via MMP-9, and YO-2 can block B6RV2 lymphoma growth. This conclusion suggests that Plg is a direct therapeutic target to tackle lymphoma.

Plg/Plm is the main enzyme among the fibrinolytc system. To test whether other fibrinolytic inhibitors are also applicable to the treatment of T-cell lymphoma, B6RV2-bearing mice were treated with tranexamic acid (TA), a synthetic derivative of the amino-acid lysine, which exerts its anti-fibrinolytic effect through the reversible blockade of lysine binding sites on Plg molecules. TA caused T-cell lymphoma growth retardation, but this effect did not reach significance (Supplementary Figure S2). TA is a drug that blocks fibrinolysis although it does not inhibit the enzymatic activity of Plm.[16] This indicates that Plg regulate T-cell lymphoma growth independently of its fibrinolytic function.

YO-2 treatment reduced the tissue infiltration of $CD45^+CD11b^+F4/80^+$ myeloid cells, and the infiltration of $F4/80^+$ cells in WT, but not in $MMP\text{-}9^{-/-}$ lymphoma-bearing mice, respectively (Figures 3e and f). Additionally, the infiltration of $CD11b^+Gr\text{-}1^+$ cells was inhibited in WT mice but not in $MMP\text{-}9^{-/-}$ mice by YO-2 treatment (Supplementary Figure S1). To identify the hematopoietic cell types within the $CD45^+CD11b^+F4/80^+$ cells derived from T-cell lymphoma tissues, we sorted $CD45^+CD11b^+F4/80^+$ cells according to their sideward light scatter (SSC) into SSC^{high} and SSC^{low} cells using FACSAria. The SSC^{high} fraction consisted of eosinophils, whereas the SSC^{low} fraction contained mainly monocytes (Figure 4a). We observed delayed tumor growth in $Plg^{-/-}$ mice injected with B6RV2 or RMA T-cell T-cell lymphoma cells, but not in mice inoculated with the EL4T cell T-cell lymphoma, Lewis lung carcinoma or B16 melanoma cells (data not shown). We mainly found eosinophils in crushed tumor tissues of B6RV2 and RMA, and monocytes in tumor tissues established using EL4, B16 and Lewis lung carcinoma cells (Figure 4b). Anti-CD11b treatment reduced T-cell lymphoma growth in WT mice and no significant further T-cell lymphoma growth retardation was observed in anti-CD11b-treated $Plg^{-/-}$ mice (Figure 4c).

In mice challenged intravenously with lymphoma cells, treatment with Plm inhibitor YO-2 prolonged the survival compared with the phosphate-buffered saline-treated group (Figure 4d), although the white blood cell counts were not significantly different between both groups (Figure 4e). Indeed, treatment of YO-2 *in vitro* did not affect lymphoma cell proliferation (data not shown). These data indicate that YO-2 improved the survival of lymphoma-inoculated mice not by suppressing the proliferation of B6RV2 cells but by modulating the local lymphoma microenvironment. Taken together, these results suggest that YO-2, a specific Plm inhibitor, can reduce T-cell lymphoma growth through regulating MMP-9-dependent $CD11b^+/F4/80^+$ myeloid cell recruitment.

Plm inhibitor blocks cytokine increase during T-cell lymphoma growth

Protease–cytokine interactions are important in the remodeling of the T-cell lymphoma microenvironment in T-cell lymphoma growth. Recent reports have indicated that tumor-infiltrating myeloid cells are a source for local cytokine release into the tumor microenvironment *in vivo* and related to tumor malignancy.[17,18] We examined T-cell lymphoma growth-associated cytokine expression in FACS-isolated $CD45^+CD11b^+F4/80^+$ cells from B6RV2-bearing T-cell lymphoma tissues (Figure 5a). Tumor-infiltrating $CD45^+CD11b^+F4/80^+$ cells expressed

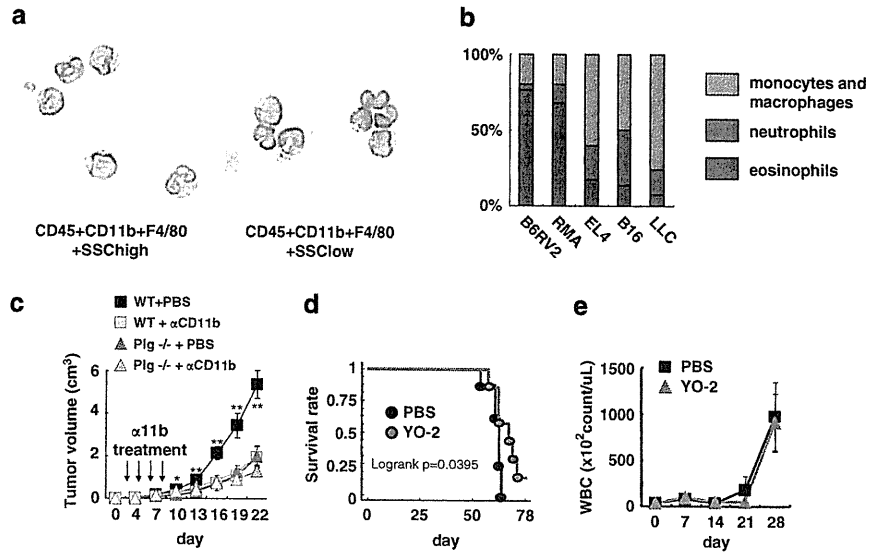

Figure 4 Lymphoma-derived $CD45^+CD11b^+F4/80^+$ cells consisted of eosinophils. (**a**, **b**) Lymphoma-derived $CD45^+CD11b^+F4/80^+$ cells were gated into SSC^{high} and SSC^{low} cells and were isolated by FACSAria. The SSC^{high} fraction consisted of eosinophils, whereas the SSC^{low} fraction mainly contained monocytes as visualized on May Grunwald-stained slides. (**b**) Relative contribution of different hematopoietic cell types within the tumor-infiltrating $CD45^+CD11b^+$ cell population isolated from various murine tumors. ($n=3$). (**c**) B6RV2-injected $Plg^{-/-}$ and WT mice were treated with anti-CD11b or control antibodies ($n=3$; $^*P<0.05$; $^{**}P<0.01$). Tumor volume was measured. (**d**) WT mice were injected intravenously with B6RV2 followed by treatment with phosphate-buffered saline or YO-2 and survival rate was observed. Statistic analysis using log rank test showed *P*-value of 0.0395 ($n=7$). (**e**) WT mice were injected intravenously with B6RV2 followed by treatment with PBS (phosphate-buffered saline) or YO-2. White blood cell (WBC) count was measured ($n=4$).

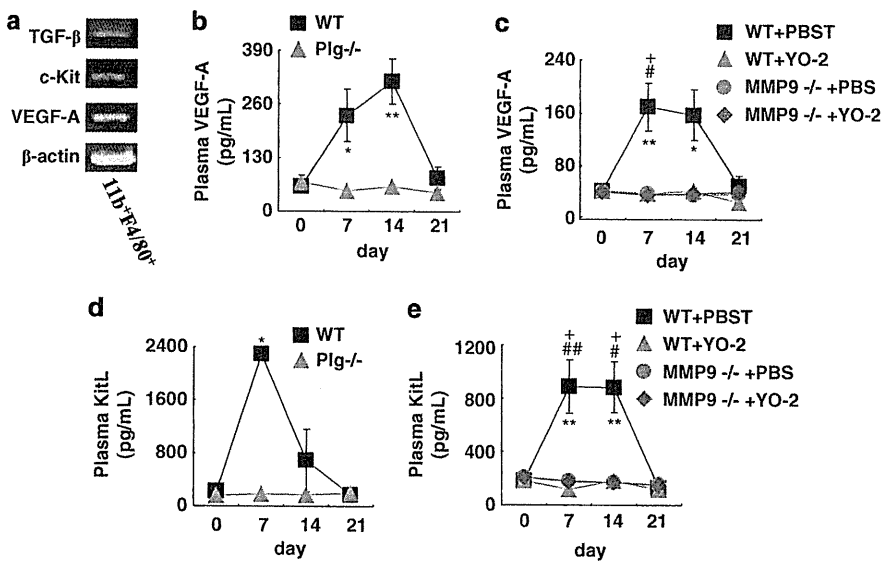

Figure 5 Plm inhibitor blocks cytokine increase during lymphoma growth. (**a**) $CD45^+CD11b^+F4/80^+$ cells were sorted out from B6RV2 lymphoma-bearing WT mice and cDNA was obtained. Reverse transcription-PCR was performed for several cytokines and receptors. The result was confirmed by repeating once. (**b**, **c**) ELISA assay of VEGF-A in plasma samples: (**b**); $n=3$; $^*P<0.05$ and $^{**}P<0.01$; (**c**); $n=3$; $^*P<0.05$ and $^{**}P<0.01$ comparing PBS-treated WT with YO-2-treated WT mice; $^{\#}P<0.05$ comparing PBS-treated WT with PBS-treated MMP-$9^{-/-}$ mice; $^{+}P<0.05$ comparing PBS-treated WT with YO-2-treated MMP-$9^{-/-}$ mice. (**d**, **e**) ELISA assay of KitL in plasma samples: (**d**) $n=3$; $^*P<0.05$, (**e**); $n=3$; $^{**}P<0.01$ comparing PBS-treated WT with YO-2-treated WT mice; $^{\#}P<0.05$ and $^{\#\#}P<0.01$ comparing PBS-treated WT with PBS-treated MMP-$9^{-/-}$ mice; $^{+}P<0.05$ comparing PBS-treated WT with YO-2-treated MMP-$9^{-/-}$ mice.

transforming growth factor-β 1, VEGF-A and c-Kit. The former factors are known to influence the survival and proliferation of T-cell lymphoma cells.[17]

Plg or MMPs can liberate VEGF-A from extracellular matrix stores.[19] Augmented plasma VEGF-A levels were observed in T-cell lymphoma-bearing WT, but not in $Plg^{-/-}$ mice (Figure 5b), in YO-2-treated WT mice, nor in MMP-$9^{-/-}$ mice with or without YO-2 treatment (Figure 5c). VEGF-A is a well-known angiogenic factor. But surprisingly, Plg deficiency did not result in reduced vessel density in B6RV2T cell lymphoma tissues when compared with WT controls (Supplementary Figure S3), implying that the reduced T-cell lymphoma growth was not due to impaired angiogenesis. It has been shown that VEGF-A induces hematopoietic cell mobilization and myeloid cell differentiation.[20,21] KitL also induces myeloid cell differentiation.[22]

Plasma KitL levels were increased in T-cell lymphoma-bearing WT, but not in $Plg^{-/-}$ mice (Figure 5d), but did not

rise in T-cell lymphoma-bearing mice with drug- or genetically-induced Plg deficiency, with MMP-9 deficiency with or without YO-2 treatment (Figure 5e). Interestingly, the peak of infiltration of $CD11b^+F4/80^+$ cells into T-cell lymphoma tissues coincided with peak plasma KitL levels in T-cell lymphoma-bearing WT mice (data not shown). Lymphoma patients show abnormal plasma levels of cytokines produced primarily by lymphoma cells or secondarily by stromal cells.[23] Myeloid cells can provide proangiogenic factors such as VEGF-A and MMP-9.[24]

VEGF-A can be liberated from extracellular matrix stores after Plg or MMP activation.[19] Our data demonstrate that Plg activation during lymphoma growth controls plasma VEGF-A levels via MMP-9 modulation. Indeed, we showed that VEGFR1 was required for myeloid cell recruitment into B6RV2 lymphoma tissues *in vivo*.[25] We have shown that activation of MMP-9 by Plm can expand the myeloid cell pool and mobilize pro-angiogenic myeloid cells, a process dependent on VEGF-A and KitL.[4] Here, our findings indicate that Plm activation during T-cell lymphoma growth increases plasma VEGF-A and KitL levels and recruits $CD11b^+F4/80^+$ cells into T-cell lymphoma tissues.

Discussion

The tumor microenvironment including immune cells, fibrosis and angiogenesis can influence the survival of lymphoma patients after treatment.[26] Our study provides *in vivo* evidence that Plg regulates T-cell lymphoma growth upstream of MMP-9, and controls both the infiltration of $CD45^+CD11b^+F4/80^+$ into T-cell lymphomas and the release of stromal cell-associated growth factors. We propose that targeted inhibition of Plg is a new therapeutic approach that can control T-cell lymphoma growth by modulating the T-cell lymphoma microenvironment.

We showed that T-cell lymphoma growth in a T-cell lymphoma model was retarded in $MMP\text{-}9^{-/-}$ mice and that Plm inhibitors failed to further decrease the already low T-cell lymphoma growth in MMP-9-deficient mice. Other protumorgenic targets of Plg aside from MMP-9 are conceivable, for example, MMP-3, as Plm also activate pro-MMP-1, pro-MMP-3 and pro-MMP13 (refs 27,28) or pro-tumorgenic growth factors and cytokines such as basic fibroblast growth factor.[29]

A study using a spontaneous T-cell lymphoma model demonstrated that MMP-9 deficiency in lymphoma cells resulted in a drop in survival time caused by increased tumor metastasis.[30] Further studies will be necessary to unravel the role of Plg and MMP in the invasion and metastasis of T-cell lymphoma cells.

As previously stated, Plm induces fibrinolysis.[2] Recently, tumor growth dependence on fibrinogen has been linked to the anatomic location of the tumor.[31] Tumor growth of Lewis lung carcinoma was sustained in $Plg^{-/-}$ mice when transplanted into the dorsal skin but was suppressed in the footpad, where vaso-occlusive thrombi occurrence limited tumor blood supply. Fibrinogen deficiency restored tumor growth in footpad-transplanted $Plg^{-/-}$ mice. How is T-cell lymphoma growth controlled by Plm/the fibrinolytic system? Plm deficiency, either genetically-induced ($Plg^{-/-}$ mice) or drug-induced (treatment with YO-2, an inhibitor of Plm), blocked T-cell lymphoma growth, indicating that Plg activation was required for T-cell lymphoma growth. YO-2 treatment inhibited T-cell lymphoma growth as efficiently as genetic deletion of Plg. Although YO-2 blocked the T-cell lymphoma growth, TA administration to the T-cell lymphoma model did not cause T-cell lymphoma growth delay (Supplementary Figure S2). TA is a drug that blocks fibrinolysis, but can accelerate Plm formation *in vitro*.[16] We therefore proposed that T-cell lymphoma growth retardation was due to the action of Plm, rather than to that of fibrinogen. Further studies will be necessary to prove this hypothesis.

Infiltrating innate immune cells support lymphoma cell survival and/or proliferation and correlate with a poor prognosis.[32] We show that $CD45^+CD11b^+F4/80^+$ myeloid cell influx requires the presence of both MMP-9 and Plm whereas infiltration of $CD11b^+Gr\text{-}1^+$ myeloid cells into T-cell lymphoma tissues is Plg dependent, but is independent of MMP-9. The importance of $CD11b^+$ cells for T-cell lymphoma growth was confirmed in the studies using neutralizing antibodies against CD11b. T-cell lymphoma growth was inhibited in WT mice and could not be further blocked in $Plg^{-/-}$ mice, indicating that the role of Plg for T-cell lymphoma growth was driven by its ability to regulate $CD11b^+$ cell migration. A role of Plg in $CD45^+$ cell migration into the medial layer of allografted vascular tissue in graft vascular disease model has been reported.[33]

Cytokines and chemokines released from tumor cells can regulate the influx of hematopoietic cells. Plg-dependent tumor inhibition was observed in tumors in which a high rate of infiltrating eosinophils had been detected. We observed increased KitL levels in lymphoma-bearing mice, which was blocked in Plg-deficient mice. KitL can recruit c-kit receptor-positive eosinophils.[34] Eotaxin, a potent eosinophil chemotactic factor promotes eosinophil transmigration via the activation of the Plg–Plm system[35] Further studies will be necessary to understand whether these or other factors released from tumor cells have a role for the observed impaired influx of myeloid cells into tumors after Plm inhibition. The role of eosinophils is controversial in different types of malignancies as both growth promoting and inhibitory effects had been described.[36] Further studies will be needed to understand the role of eosinophils in T-cell lymphoma and to establish a role for Plg in the regulation of other eosinophilia-associated diseases. In our model, $CD45^+CD11b^+F4/80^+$ cells expressed cytokines such as VEGF-A and transforming growth factor-β. These factors are known to accelerate lymphoma growth.[37] These studies support our findings that myeloid cell infiltration is dependent on the activation of the Plg/MMP-9 pathway. Furthermore, multiple reports have shown that myeloid cells mediate key steps of tumor progression.[38]

In conclusion, we show that the Plg/MMP-9 pathway can regulate T-cell lymphoma growth and accelerate the recruitment of T-cell lymphoma growth supportive $CD45^+CD11b^+F4/80^+$ myeloid cells into T-cell lymphoma tissues. Therefore, targeting the Plg/MMP-9 pathway (for example, using YO-2) should offer a new approach for therapeutic intervention in lymphoid malignancy.

Conflict of interest

The authors declare no conflict of interest.

Acknowledgements

We thank Stephanie C Napier, H Tachikawa, and A Furuhata (Juntendo University) and the FACS core facility for their help. Human recombinant tissue-type Plg activator was provided by the Eisai corporation (Japan). This work was supported by the Japan Society for the Promotion of Science and Grants-in-Aid for Scientific Research from the Ministry of Education, Culture, Sports, Science and Technology (MEXT) (KH; BH); grants from the Ministry of Health, Labour and Welfare (KH), Mitsubishi

Pharma Research Foundation (KH), Kyowa Hakko Kirin Co., Ltd (KH), Japan Leukaemia Research Fund (KH), Novartis Foundation (BH) and Sagawa Foundation (BH); Program for Improvement of the Research Environment for Young Researchers (BH) funded by the Special Coordination Funds for Promoting Science and Technology of the MEXT, Japan.

References

1 Huber K, Kirchheimer JC, Sedlmayer A, Bell C, Ermler D, Binder BR. Clinical value of determination of urokinase-type plasminogen activator antigen in plasma for detection of colorectal cancer: comparison with circulating tumor-associated antigens CA 19-9 and carcinoembryonic antigen. *Cancer Res* 1993; **53**: 1788–1793.
2 Dano K, Behrendt N, Hoyer-Hansen G, Johnsen M, Lund LR, Ploug M *et al.* Plasminogen activation and cancer. *Thromb Haemost* 2005; **93**: 676–681.
3 Thomas GT, Lewis MP, Speight PM. Matrix metalloproteinases and oral cancer. *Oral Oncol* 1999; **35**: 227–233.
4 Heissig B, Lund LR, Akiyama H, Ohki M, Morita Y, Romer J *et al.* The plasminogen fibrinolytic pathway is required for hematopoietic regeneration. *Cell Stem Cell* 2007; **1**: 658–670.
5 Hazar B, Polat G, Seyrek E, Bagdatoglglu O, Kanik A, Tiftik N. Prognostic value of matrix metalloproteinases (MMP-2 and MMP-9) in Hodgkin's and non-Hodgkin's lymphoma. *Int J Clin Pract* 2004; **58**: 139–143.
6 Johansson M, Denardo DG, Coussens LM. Polarized immune responses differentially regulate cancer development. *Immunol Rev* 2008; **222**: 145–154.
7 Ruan J, Hajjar K, Rafii S, Leonard JP. Angiogenesis and antiangiogenic therapy in non-Hodgkin's lymphoma. *Ann Oncol* 2009; **20**: 413–424.
8 Van Lint P, Libert C. Chemokine and cytokine processing by matrix metalloproteinases and its effect on leukocyte migration and inflammation. *J Leukoc Biol* 2007; **82**: 1375–1381.
9 Coussens LM, Tinkle CL, Hanahan D, Werb Z. MMP-9 supplied by bone marrow-derived cells contributes to skin carcinogenesis. *Cell* 2000; **103**: 481–490.
10 Okada Y, Tsuda Y, Wanaka K, Tada M, Okamoto U, Okamoto S *et al.* Development of plasmin and plasma kallikrein selective inhibitors and their effect on M1 (melanoma) and HT29 cell lines. *Bioorg Med Chem Lett* 2000; **10**: 2217–2221.
11 Bugge TH, Flick MJ, Daugherty CC, Degen JL. Plasminogen deficiency causes severe thrombosis but is compatible with development and reproduction. *Genes Dev* 1995; **9**: 794–807.
12 Nakayama E, Uenaka A, Stockert E, Obata Y. Detection of a unique antigen on radiation leukemia virus-induced leukemia B6RV2. *Cancer Res* 1984; **44**: 5138–5144.
13 Jin DK, Shido K, Kopp HG, Petit I, Shmelkov SV, Young LM *et al.* Cytokine-mediated deployment of SDF-1 induces revascularization through recruitment of CXCR4+ hemangiocytes. *Nat Med* 2006; **12**: 557–567.
14 Shojaei F, Wu X, Malik AK, Zhong C, Baldwin ME, Schanz S *et al.* Tumor refractoriness to anti-VEGF treatment is mediated by $CD11b^{+}Gr1^{+}$ myeloid cells. *Nat Biotechnol* 2007; **25**: 911–920.
15 Lin EY, Li JF, Gnatovskiy L, Deng Y, Zhu L, Grzesik DA *et al.* Macrophages regulate the angiogenic switch in a mouse model of breast cancer. *Cancer Res* 2006; **66**: 11238–11246.
16 Longstaff C. Studies on the mechanisms of action of aprotinin and tranexamic acid as plasmin inhibitors and antifibrinolytic agents. *Blood Coagul Fibrinolysis* 1994; **5**: 537–542.
17 Zhao WL, Mourah S, Mounier N, Leboeuf C, Daneshpouy ME, Legres L *et al.* Vascular endothelial growth factor-A is expressed both on lymphoma cells and endothelial cells in angioimmunoblastic T-cell lymphoma and related to lymphoma progression. *Lab Invest* 2004; **84**: 1512–1519.
18 Kadin ME, Cavaille-Coll MW, Gertz R, Massague J, Cheifetz S, George D. Loss of receptors for transforming growth factor beta in human T-cell malignancies. *Proc Natl Acad Sci USA* 1994; **91**: 6002–6006.
19 Heissig B, Hattori K, Friedrich M, Rafii S, Werb Z. Angiogenesis: vascular remodeling of the extracellular matrix involves metalloproteinases. *Curr Opin Hematol* 2003; **10**: 136–141.
20 Lyden D, Hattori K, Dias S, Costa C, Blaikie P, Butros L *et al.* Impaired recruitment of bone-marrow-derived endothelial and hematopoietic precursor cells blocks tumor angiogenesis and growth. *Nat Med* 2001; **7**: 1194–1201.
21 Heissig B, Rafii S, Akiyama H, Ohki Y, Sato Y, Rafael T *et al.* Low-dose irradiation promotes tissue revascularization through VEGF release from mast cells and MMP-9-mediated progenitor cell mobilization. *J Exp Med* 2005; **202**: 739–750.
22 Heissig B, Hattori K, Dias S, Friedrich M, Ferris B, Hackett NR *et al.* Recruitment of stem and progenitor cells from the bone marrow niche requires MMP-9 mediated release of kit-ligand. *Cell* 2002; **109**: 625–637.
23 Doussis-Anagnostopoulou IA, Talks KL, Turley H, Debnam P, Tan DC, Mariatos G *et al.* Vascular endothelial growth factor (VEGF) is expressed by neoplastic Hodgkin-Reed-Sternberg cells in Hodgkin's disease. *J Pathol* 2002; **197**: 677–683.
24 Rafii S, Lyden D, Benezra R, Hattori K, Heissig B. Vascular and haematopoietic stem cells: novel targets for anti-angiogenesis therapy? *Nat Rev Cancer* 2002; **2**: 826–835.
25 Kaplan RN, Riba RD, Zacharoulis S, Bramley AH, Vincent L, Costa C *et al.* VEGFR1-positive haematopoietic bone marrow progenitors initiate the pre-metastatic niche. *Nature* 2005; **438**: 820–827.
26 Lenz G, Wright G, Dave SS, Xiao W, Powell J, Zhao H *et al.* Stromal gene signatures in large-B-cell lymphomas. *N Engl J Med* 2008; **359**: 2313–2323.
27 Okada Y, Gonoji Y, Naka K, Tomita K, Nakanishi I, Iwata K *et al.* Matrix metalloproteinase 9 (92-kDa gelatinase/type IV collagenase) from HT 1080 human fibrosarcoma cells. Purification and activation of the precursor and enzymic properties. *J Biol Chem* 1992; **267**: 21712–21719.
28 Suzuki K, Enghild JJ, Morodomi T, Salvesen G, Nagase H. Mechanisms of activation of tissue procollagenase by matrix metalloproteinase 3 (stromelysin). *Biochemistry* 1990; **29**: 10261–10270.
29 Lyons RM, Keski-Oja J, Moses HL. Proteolytic activation of latent transforming growth factor-beta from fibroblast-conditioned medium. *J Cell Biol* 1988; **106**: 1659–1665.
30 Roy JS, Van Themsche C, Demers M, Opdenakker G, Arnold B, St-Pierre Y. Triggering of T-cell leukemia and dissemination of T-cell lymphoma in MMP-9-deficient mice. *Leukemia* 2007; **21**: 2506–2511.
31 Palumbo JS, Talmage KE, Liu H, La Jeunesse CM, Witte DP, Degen JL. Plasminogen supports tumor growth through a fibrinogen-dependent mechanism linked to vascular patency. *Blood* 2003; **102**: 2819–2827.
32 de Jong D, Enblad G. Inflammatory cells and immune microenvironment in malignant lymphoma. *J Intern Med* 2008; **264**: 528–536.
33 Moons L, Shi C, Ploplis V, Plow E, Haber E, Collen D *et al.* Reduced transplant arteriosclerosis in plasminogen-deficient mice. *J Clin Invest* 1998; **102**: 1788–1797.
34 Lukacs N, Strieter R, Lincoln P, Brownell E, Pullen D, Schock H *et al.* Stem cell factor (c-kit ligand) influences eosinophil recruitment and histamine levels in allergic airway inflammation. *J Immunol* 1996; **156**: 3945–3951.
35 Ferland C, Guilbert M, Davoine F, Flamand N, Chakir J, Laviolette M. Eotaxin promotes eosinophil transmigration via the activation of the plasminogen-plasmin system. *J Leukoc Biol* 2001; **69**: 772–778.
36 Martinelli-Klay CP, Mendis BR, Lombardi T. Eosinophils and oral squamous cell carcinoma: a short review. *J Oncol* 2009; **2009**: 310132.
37 Reimann M, Lee S, Loddenkemper C, Dorr JR, Tabor V, Aichele P *et al.* Tumor stroma-derived TGF-beta limits myc-driven lymphomagenesis via Suv39h1-dependent senescence. *Cancer Cell* 2010; **17**: 262–272.
38 Lin EY, Nguyen AV, Russell RG, Pollard JW. Colony-stimulating factor 1 promotes progression of mammary tumors to malignancy. *J Exp Med* 2001; **193**: 727–740.

Supplementary Information accompanies the paper on the Leukemia website (http://www.nature.com/leu)

ARTICLE

doi:10.1038/nature10496

Frequent pathway mutations of splicing machinery in myelodysplasia

Kenichi Yoshida[1]*, Masashi Sanada[1]*, Yuichi Shiraishi[2]*, Daniel Nowak[3]*, Yasunobu Nagata[1]*, Ryo Yamamoto[4], Yusuke Sato[1], Aiko Sato-Otsubo[1], Ayana Kon[1], Masao Nagasaki[5], George Chalkidis[6], Yutaka Suzuki[7], Masashi Shiosaka[1], Ryoichiro Kawahata[1], Tomoyuki Yamaguchi[8], Makoto Otsu[4], Naoshi Obara[9], Mamiko Sakata-Yanagimoto[9], Ken Ishiyama[10], Hiraku Mori[11], Florian Nolte[3], Wolf-Karsten Hofmann[3], Shuichi Miyawaki[10], Sumio Sugano[7], Claudia Haferlach[12], H. Phillip Koeffler[13,14], Lee-Yung Shih[15], Torsten Haferlach[12], Shigeru Chiba[9], Hiromitsu Nakauchi[4,8], Satoru Miyano[2,6] & Seishi Ogawa[1]

Myelodysplastic syndromes and related disorders (myelodysplasia) are a heterogeneous group of myeloid neoplasms showing deregulated blood cell production with evidence of myeloid dysplasia and a predisposition to acute myeloid leukaemia, whose pathogenesis is only incompletely understood. Here we report whole-exome sequencing of 29 myelodysplasia specimens, which unexpectedly revealed novel pathway mutations involving multiple components of the RNA splicing machinery, including *U2AF35*, *ZRSR2*, *SRSF2* and *SF3B1*. In a large series analysis, these splicing pathway mutations were frequent (~45 to ~85%) in, and highly specific to, myeloid neoplasms showing features of myelodysplasia. Conspicuously, most of the mutations, which occurred in a mutually exclusive manner, affected genes involved in the 3′-splice site recognition during pre-mRNA processing, inducing abnormal RNA splicing and compromised haematopoiesis. Our results provide the first evidence indicating that genetic alterations of the major splicing components could be involved in human pathogenesis, also implicating a novel therapeutic possibility for myelodysplasia.

Myelodysplastic syndromes (MDS) and related disorders (myelodysplasia) comprise a group of myeloid neoplasms characterized by deregulated, dysplastic blood cell production and a predisposition to acute myeloid leukaemia (AML)[1]. Although the prevalence of MDS has not been determined precisely, more than 10,000 people are estimated to develop myelodysplasia annually in the United States[2]. Their indolent clinical course before leukaemic transformation and ineffective haematopoiesis with evidence of myeloid dysplasia indicate a pathogenesis distinct from that involved in *de novo* AML. Currently, a number of gene mutations and cytogenetic changes have been implicated in the pathogenesis of MDS, including mutations of *RAS*, *TP53* and *RUNX1*, and more recently *ASXL1*, *c-CBL*, *DNMT3A*, *IDH1/2*, *TET2* and *EZH2* (ref. 3). Nevertheless, mutations of this set of genes do not fully explain the pathogenesis of MDS because they are also commonly found in other myeloid malignancies and roughly 20% of MDS cases have no known genetic changes (ref. 4 and unpublished data). In particular, the genetic alterations responsible for the dysplastic phenotypes and ineffective haematopoiesis of myelodysplasia are poorly understood. Meanwhile, the recent development of massively parallel sequencing technologies has provided an expanded opportunity to discover genetic changes across the entire genomes or protein-coding sequences in human cancers at a single-nucleotide level[5–10], which could be successfully applied to the genetic analysis of myelodysplasia to obtain a better understanding of its pathogenesis.

Overview of genetic alterations

In this study, we performed whole-exome sequencing of paired tumour/control DNA from 29 patients with myelodysplasia (Supplementary Table 1). Although incapable of detecting non-coding mutations and gene rearrangements, the whole-exome approach is a well-established strategy for obtaining comprehensive registries of protein-coding mutations at low cost and high performance. With a mean coverage of 133.8, 80.4% of the target sequences were analysed at more than ×20 depth on average (Supplementary Fig. 1). All the candidates for somatic mutations ($N = 497$) generated through our data analysis pipeline were subjected to validation using Sanger sequencing (Supplementary Methods I and Supplementary Fig. 2). Finally, 268 non-synonymous somatic mutations were confirmed with an overall true positive rate of 53.9% (Supplementary Fig. 3), including 206 missense, 25 nonsense, and 10 splice site mutations, and 27 frameshift-causing insertions/deletions (indels) (Supplementary Fig. 4). The mutation rate of 9.2 (0–21) per sample was significantly lower than that in solid tumours (16.2–302)[7,11,12] and multiple myeloma (32.4)[6], but was comparable to that in AML (7.3–13)[13–15] and chronic lymphocytic leukaemia (11.5)[16]. Combined with the genomic copy number profile obtained by single nucleotide polymorphism (SNP) array karyotyping, this array of somatic mutations provided a landscape of myelodysplasia genomes (Supplementary Fig. 5)[17,18].

[1]Cancer Genomics Project, Graduate School of Medicine, The University of Tokyo, 7-3-1 Hongo, Bunkyo-ku, Tokyo 113-8655, Japan. [2]Laboratory of DNA Information Analysis, Human Genome Center, Institute of Medical Science, The University of Tokyo, 4-6-1 Shirokanedai, Minato-ku, Tokyo 108-8639, Japan. [3]Department of Hematology and Oncology, Medical Faculty Manheim of the University of Heidelberg, 1–3 Theodor-Kutzer-Ufer, Mannheim 68167, Germany. [4]Division of Stem Cell Therapy, Center for Stem Cell Biology and Regenerative Medicine, Institute of Medical Science, The University of Tokyo, 4-6-1 Shirokanedai, Minato-ku, Tokyo 108-8639, Japan. [5]Laboratory of Functional Genomics, Human Genome Center, Institute of Medical Science, The University of Tokyo, 4-6-1 Shirokanedai, Minato-ku, Tokyo 108-8639, Japan. [6]Laboratory of Sequence Data Analysis, Human Genome Center, Institute of Medical Science, The University of Tokyo, 4-6-1 Shirokanedai, Minato-ku, Tokyo 108-8639, Japan. [7]Division of Systems Biomedical Technology, Institute of Medical Science, The University of Tokyo, 4-6-1 Shirokanedai, Minato-ku, Tokyo 108-8639, Japan. [8]Nakauchi Stem Cell and Organ Regeneration Project, Exploratory Research for Advanced Technology, Japan Science and Technology Agency, 4-6-1 Shirokanedai, Minato-ku, Tokyo 108-8639, Japan. [9]Department of Hematology, Institute of Clinical Medicine, University of Tsukuba, 1-1-1 Tennodai, Tsukuba-shi, Ibaraki, 305-8571, Japan. [10]Division of Hematology, Tokyo Metropolitan Ohtsuka Hospital, 2-8-1 Minami-Ohtsuka, Toshima-ku, Tokyo 170-0005, Japan. [11]Division of Hematology, Internal Medicine, Showa University Fujigaoka Hospital, 1-30 Fujigaoka, Aoba-ku, Yokohama, Kanagawa 227-8501, Japan. [12]Munich Leukemia Laboratory, Max-Lebsche-Platz 31, Munich 81377, Germany. [13]Hematology/Oncology, Cedars-Sinai Medical Center, 8700 Beverly Blvd, Los Angeles, California 90048, USA. [14]National University of Singapore, Cancer Science Institute of Singapore, 28 Medical Drive, Singapore 117456, Singapore. [15]Division of Hematology-Oncology, Department of Internal Medicine, Chang Gung Memorial Hospital, Chang Gung University, 199 Tung Hwa North Rd, Taipei 105, Taiwan.
*These authors contributed equally to this work.

Novel gene targets in myelodysplasia

The list of the somatic mutations (Supplementary Table 2) included most of the known gene targets in myelodysplasia with similar mutation frequencies to those previously reported, indicating an acceptable sensitivity of the current study. The mutations of the known gene targets, however, accounted for only 12.3% of all detected mutations ($N = 33$), and the remaining 235 mutations involved previously unreported genes. Among these, recurrently mutated genes in multiple cases are candidate targets of particular interest, for which high mutation rates are expected in general populations. In fact, 8 of the 12 recurrently mutated genes were among the well-described gene targets in myelodysplasia (Supplementary Table 3). However, what immediately drew our attention were the recurrent mutations involving *U2AF35* (also known as *U2AF1*), *ZRSR2* and *SRSF2* (*SC35*), because they belong to the common pathway known as RNA splicing. Including an additional three genes mutated in single cases (*SF3A1*, *SF3B1* and *PRPF40B*), six components of the splicing machinery were mutated in 16 out of the 29 cases (55.2%) in a mutually exclusive manner (Fig. 1, Supplementary Fig. 6 and Supplementary Table 2).

Frequent mutations in splicing machinery

RNA splicing is accomplished by a well-ordered recruitment, rearrangement and/or disengagement of a set of small nuclear ribonucleoprotein (snRNP) complexes (U1, U2, and either U4/5/6 or U11/12), as well as many other protein components onto the pre-mRNAs. Notably, the mutated components of the spliceosome were all engaged in the initial steps of RNA splicing, except for PRPF40B, whose functions in RNA splicing are poorly defined. Making physical interactions with SF1 and a serine/arginine-rich (SR) protein, such as SRSF1 or SRSF2, the U2 auxiliary factor (U2AF) that consists of the U2AF65 (U2AF2)–U2AF35 heterodimer, is involved in the recognition of the 3′ splice site (3′SS) and its nearby polypyrimidine tract, which is thought to be required for the subsequent recruitment of the U2 snRNP, containing SF3A1 as well as SF3B1, to establish the splicing A complex (Fig. 1)[19]. ZRSR2 (or Urp), is another essential component of the splicing machinery. Showing a close structural similarity to U2AF35, ZRSR2 physically interacts with U2AF65, as well as SRSF1 and SRSF2, with a distinct function from its homologue, U2AF35 (ref. 20).

To confirm and extend the initial findings in the whole-exome sequencing, we studied mutations of the above six genes together with three additional spliceosome-related genes, including *U2AF65*, *SF1* and *SRSF1*, in a large series of myeloid neoplasms ($N = 582$) using a high-throughput mutation screen of pooled DNA followed by confirmation/identification of candidate mutations (refs 21 and 22 and Supplementary Methods II).

In total, 219 mutations were identified in 209 out of the 582 specimens of myeloid neoplasms through validating 313 provisional positive events in the pooled DNA screen (Supplementary Tables 4 and 5). The mutations among four genes, *U2AF35* ($N = 37$), *SRSF2* ($N = 56$), *ZRSR2* ($N = 23$) and *SF3B1* ($N = 79$), explained most of the mutations with much lower mutational rates for *SF3A1* ($N = 8$), *PRPF40B* ($N = 7$), *U2AF65* ($N = 4$) and *SF1* ($N = 5$) (Fig. 2). Mutations of the splicing machinery were highly specific to diseases showing myelodysplastic features, including MDS either with (84.9%) or without (43.9%) increased ring sideroblasts, chronic myelomonocytic leukaemia (CMML) (54.5%), and therapy-related AML or AML with myelodysplasia-related changes (25.8%), but were rare in *de novo* AML (6.6%) and myeloproliferative neoplasms (MPN) (9.4%) (Fig. 3a). The mutually exclusive pattern of the mutations in these splicing pathway genes was confirmed in this large case series, suggesting a common impact of these mutations on RNA splicing and the pathogenesis of myelodysplasia (Fig. 3b). The frequencies of mutations showed significant differences across disease types. Surprisingly, *SF3B1* mutations were found in the majority of the cases with MDS characterized by increased ring sideroblasts, that is, refractory anaemia with ring sideroblasts (RARS) (19/23 or 82.6%) and refractory cytopenia with multilineage dysplasia with ≥ 15% ring sideroblasts (RCMD-RS) (38/50 or 76%) with much lower mutation frequencies in other myeloid neoplasms. RARS and RCMD-RS account

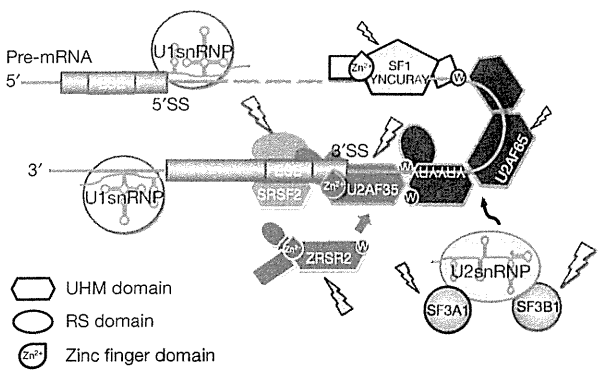

Figure 1 | Components of the splicing E/A complex mutated in myelodysplasia. RNA splicing is initiated by the recruitment of U1 snRNP to the 5′SS. SF1 and the larger subunit of the U2 auxiliary factor (U2AF), U2AF65, bind the branch point sequence (BPS) and its downstream polypyrimidine tract, respectively. The smaller subunit of U2AF (U2AF35) binds to the AG dinucleotide of the 3′SS, interacting with both U2AF65 and a SR protein, such as SRSF2, through its UHM and RS domain, comprising the earliest splicing complex (E complex). ZRSR2 also interacts with U2AF and SR proteins to perform essential functions in RNA splicing. After the recognition of the 3′SS, U2 snRNP, together with SF3A1 and SF3B1, is recruited to the 3′SS to generate the splicing complex A. The mutated components in myelodysplasia are indicated by arrows.

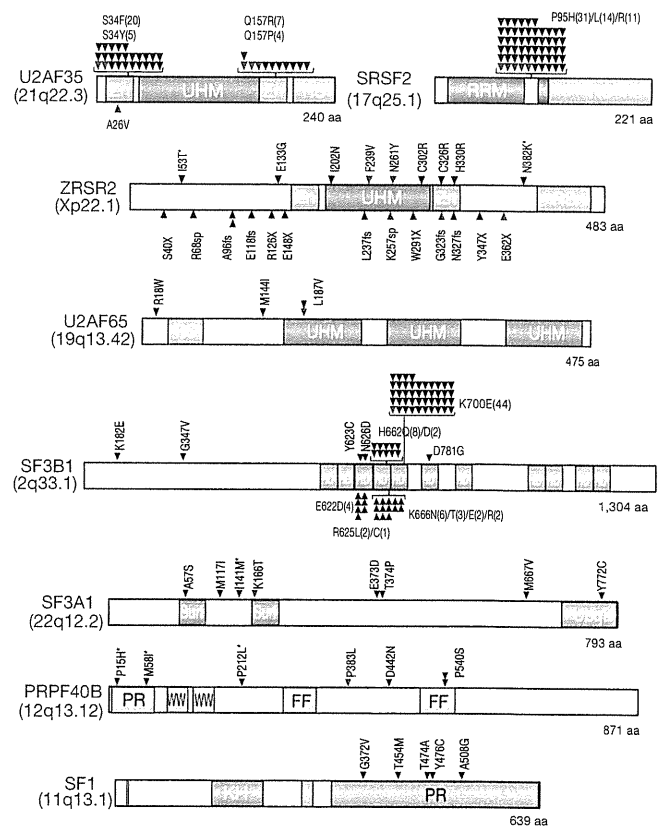

Figure 2 | Mutations of multiple components of the splicing machinery. Each mutation in the eight spliceosome components is shown with an arrowhead. Confirmed somatic mutations are discriminated by red arrows. Known domain structures are shown in coloured boxes as indicated. Mutations predicted as SNPs by MutationTaster (http://www.mutationtaster.org/) are indicated by asterisks. The number of each mutation is indicated in parenthesis. ZRSR2 mutations in females are shown in blue.

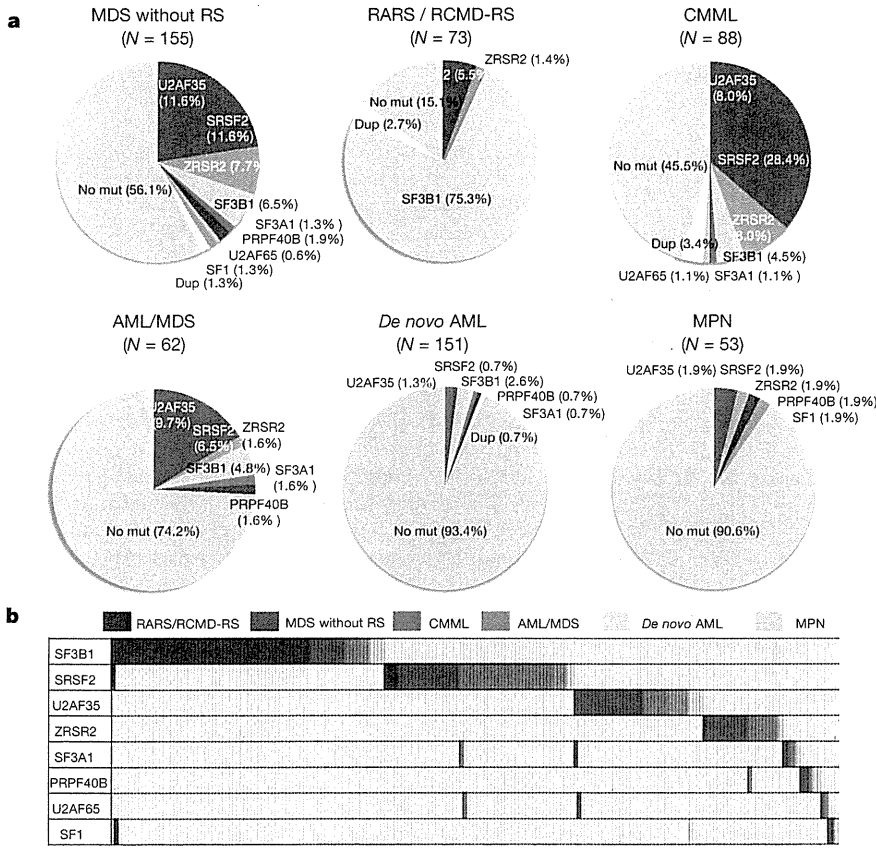

Figure 3 | Frequencies and distribution of spliceosome pathway gene mutations in myeloid neoplasms. a, Frequencies of spliceosome pathway mutations among 582 cases with various myeloid neoplasms. **b**, Distribution of mutations in eight spliceosome genes, where diagnosis of each sample is shown by indicated colours.

for 4.3% and 12.9% of MDS cases, respectively, where deregulated iron metabolism has been implicated in the development of refractory anaemia[23]. With such high mutation frequencies and specificity, the *SF3B1* mutations were thought to be almost pathognomonic to these MDS subtypes characterized by increased ring sideroblasts, and strongly implicated in the pathogenesis of MDS in these categories. Less conspicuously but significantly, *SRSF2* mutations were more frequent in CMML cases (Fig. 3 and Supplementary Table 4). Thus, although commonly involving the E/A splicing complexes, different mutations may still have different impacts on cell functions, contributing to the determination of discrete disease phenotypes. For example, studies have demonstrated that *SRSF2* was also involved in the regulation of DNA stability and that depletion of SRSF2 can lead to genomic instability[24]. Of interest in this context, regardless of disease subtypes, samples with *SRSF2* mutations were shown to have significantly more mutations of other genes compared with *U2AF35* mutations ($P = 0.001$, multiple regression analysis) (Supplementary Table 6 and Supplementary Fig. 7).

Notably, with a rare exception of A26V in a single case, the mutations of U2AF35 exclusively involved two highly conserved amino acid positions (S34 or Q157) within the amino- and the carboxyl-terminal zinc finger motifs flanking the U2AF homology motif (UHM) domain. SRSF2 mutations exclusively occurred at P95 within an intervening sequence between the RNA recognition motif (RRM) and arginine/serine-rich (RS) domains (Fig. 2 and Supplementary Figs 8 and 9). Similarly, SF3B1 mutations predominantly involved K700 and, to a lesser extent, K666, H662 and E622, which are also conserved across species (Fig. 2 and Supplementary Fig. 10). The involvement of recurrent amino acid positions in these spliceosome genes strongly indicated a gain-of-function nature of these mutations, which has been a well-documented scenario in other oncogenic mutations[25]. On the other hand, the 23 mutations in *ZRSR2* (Xp22.1) were widely distributed along the entire coding region (Fig. 2). Among these, 14 mutations were nonsense or frameshift changes, or involved splicing donor/acceptor sites that caused either a premature truncation or a large structural change of the protein, leading to loss-of-function. Combined with their strong male preference for the mutation (14/14 cases), *ZRSR2* most likely acts as a tumour suppressor gene with an X-linked recessive mode of genetic action. The remaining nine *ZRSR2* mutations were missense changes and found in both males (six cases) and females (three cases), whose somatic origin was only confirmed in two cases. However, neither the dbSNP database (build131 and 132) nor the 1000 Genomes database (May 2011 snp calls) contained these missense nucleotides, suggesting that many, if not all, of these missense changes are likely to represent functional somatic changes, especially those found in males. Interrogation of these hot spots for mutations in *U2AF35* and *SRSF2* found no mutations among lymphoid neoplasms, including acute lymphoblastic leukaemia ($N = 24$) or non-Hodgkin's lymphoma ($N = 87$) (data not shown).

RNA splicing and spliceosome mutations

Because the splicing pathway mutations in myelodysplasia widely and specifically affect the major components of the splicing complexes E/A in a mutually exclusive manner, the common consequence of these mutations is logically the impaired recognition of 3′SSs that would lead to the production of aberrantly spliced mRNA species. To appreciate this and also to gain an insight into the biological/biochemical impact of these splicing mutations, we expressed the wild-type and the mutant (S34F) U2AF35 in HeLa cells using retrovirus-mediated gene transfer with enhanced green fluorescent protein (EGFP) marking (Fig. 4a and Supplementary Methods III) and examined their effects on gene expression in these cells using GeneChip Human genome U133 plus 2.0 arrays (Affymetrix), followed by gene set enrichment analysis (GSEA) (Supplementary Methods IV)[26]. Intriguingly, the GSEA disclosed a significant enrichment of the genes on the nonsense-mediated mRNA decay (NMD) pathway among the significantly upregulated genes in mutant *U2AF35*-transduced HeLa cells (Fig. 4b, Supplementary Fig. 11a and Supplementary Table 7), which was

confirmed by quantitative polymerase chain reactions (qPCR) (Fig. 4c and Supplementary Methods 5V). A similar result was also observed for the gene expression profile of an MDS-derived cell line (TF-1) transduced with the S34F mutant (Supplementary Figs 11b, c). The NMD activation by the mutant U2AF35 was suppressed significantly by the co-overexpression of the wild-type protein (Supplementary Fig. 11d), indicating that the effect of the mutant protein was likely to be mediated by inhibition of the functions of the wild-type protein. Given that the NMD pathway, known as mRNA surveillance, provides a post-transcriptional mechanism for recognizing and eliminating abnormal transcripts that prematurely terminate translation[27], the result of the GSEA analyses indicated that the mutant U2AF35 induced abnormal RNA splicing in HeLa and TF-1 cells, leading to the generation of unspliced RNA species having a premature stop codon and induction of the NMD activity.

To confirm this, we next performed whole transcriptome analysis in these cells using the GeneChip Human exon 1.0 ST Array (Affymetrix), in which we differentially tracked the behaviour of two discrete sets of probes showing different level of evidence of being exons, that is, 'Core' (authentic exons) and 'non-Core' (more likely introns) sets (Supplementary Methods IV and Supplementary Fig. 12). As shown in Fig. 4d, the Core and non-Core set probes were differentially enriched among probes showing significant difference in expression between wild-type and mutant-transduced cells (false discovery rate (FDR) = 0.01). The Core set probes were significantly enriched in those probes significantly downregulated in mutant *U2AF35*-transduced cells compared with wild-type *U2AF35*-transduced cells, whereas the non-Core set probes were enriched in those probes significantly upregulated in mutant *U2AF35*-transduced cells (Fig. 4e). The significant differential enrichment was also demonstrated, even when all probe sets were included (Fig. 4f). Moreover, the significantly differentially expressed Core set probes tended to be up- and downregulated in wild-type and mutant *U2AF35*-transduced cells compared with mock-transduced cells, respectively, and vice versa for the differentially expressed non-Core set probes (Fig. 4e). Combined, these exon array results indicated that the wild-type U2AF35 correctly promoted authentic RNA splicing, whereas the mutant U2AF35 inhibited this processes, rendering non-Core and therefore, more likely intronic sequences to remain unspliced.

The abnormal splicing in mutant *U2AF35*-transduced cells was more directly demonstrated by sequencing mRNAs extracted from HeLa cells, in which expression of the wild-type and mutant (S34F) U2AF35 were induced by doxycycline. First, after adjusting by the total number of mapped reads, the wild-type *U2AF35*-transduced cells showed an increased read counts in the exon fraction, but reduced counts in other fractions, compared with mutant *U2AF35*-transduced cells (Fig. 4g). The reads from the mutant-transduced cells were mapped to broader genomic regions compared with those from the wild-type *U2AF35*-transduced cells, which were largely explained by non-exon reads (Fig. 4h). Finally, the number of those reads that encompassed the authentic exon/intron junctions was significantly increased in mutant *U2AF35*-transduced cells compared with wild-type *U2AF35*-transduced cells (Fig. 4i and Supplementary Methods VI). These results clearly demonstrated that failure of splicing ubiquitously occurred in mutant *U2AF35*-transduced cells. A typical example of abnormal splicing in mutant-transduced cells and the list of significantly unspliced exons are shown in Supplementary Fig. 13 and Supplementary Table 8, respectively.

Biological consequence of U2AF35 mutations

Finally, we examined the biological effects of compromised functions of the E/A splicing complexes. First, TF-1 and HeLa cells were transduced with lentivirus constructs expressing either the S34F U2AF35 mutant or wild-type U2AF35 under a tetracycline-inducible promoter (Fig. 5a and Supplementary Figs 14a and 15a), and cell proliferation was examined after the induction of their expression. Unexpectedly, after the induction of gene expression with

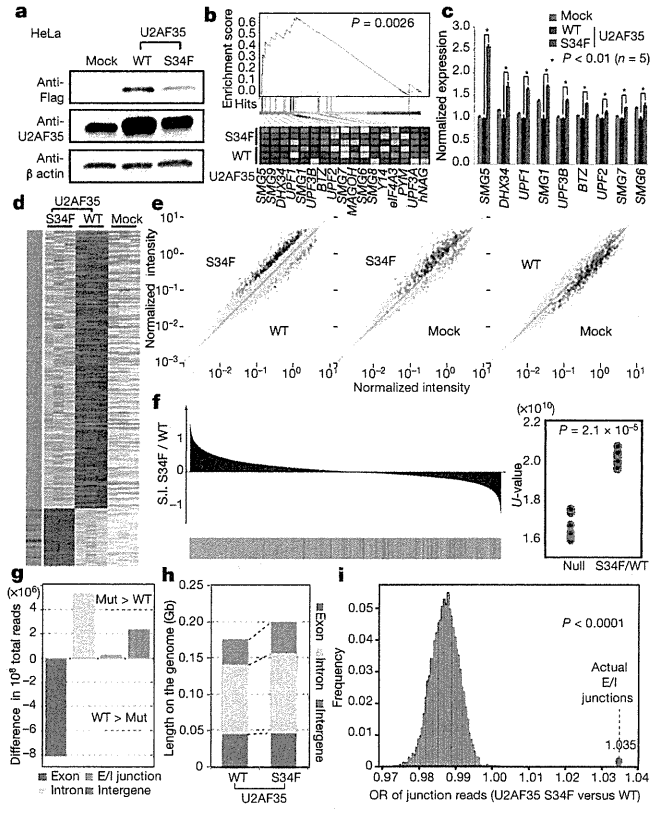

Figure 4 | Altered RNA splicing caused by a U2AF35 mutant. **a**, Western blot analyses showing expression of transduced wild-type or mutant (S34F) U2AF35 in HeLa cells used for the analyses of expression and exon microarrays. **b**, The GSEA demonstrating a significant enrichment of the set of 17 NMD pathway genes among significantly differentially expressed genes between wild-type and mutant *U2AF35*-transduced HeLa cells. The significance of the gene set was empirically determined by 1,000 gene-set permutations. **c**, The confirmation of the microarray analysis for the expression of nine genes that contributed to the core enrichment in the NMD gene set. Means ± s.e. are provided for the indicated NMD genes. *P* values were determined by the Mann–Whitney *U* test. **d**, Significantly upregulated and downregulated probe sets (FDR = 0.01) in mutant *U2AF35*-transduced cells compared with wild-type *U2AF35*-transduced cells in triplicate exon array experiments are shown in a heat map. The origin of each probe set is depicted in the left lane, where red and green bars indicate the Core and non-Core sets, respectively. **e**, Pair-wise scatter plots of the normalized intensities of entire probe sets (grey) across different experiments. The Core and non-Core set probes that were significantly differentially expressed between the wild-type and mutant *U2AF35*-transduced cells are plotted in red and green, respectively. **f**, Distribution of the Core (red) and non-Core (green) probe sets within the entire probe sets ordered by splicing index (S.I.; Supplementary Methods IV), calculated between wild-type and mutant *U2AF35*-transduced cells. In the right panel, the differential enrichment of both probe sets was confirmed by Mann–Whitney *U* test. **g**, Difference in read counts for the indicated fractions per 10^8 total reads in RNA sequencing between wild-type and mutant U2AF35-expressing HeLa cells analysis. Increased/decreased read counts in mutant U2AF35-expressing cells are plotted upward/downward, respectively. **h**, Comparison of the genome coverage by the indicated fractions in wild-type- and mutant-U2AF35-expressing cells. The genome coverage was calculated for each fraction within the 10^8 reads randomly selected from the total reads and averaged for ten independent selections. **i**, The odds ratio of the junction reads within the total mapped reads was calculated between the two experiments (red circle), which was evaluated against the 10,000 simulated values under the null hypothesis (histogram in blue).

doxycycline, the mutant *U2AF35*-transduced cells, but not the wild-type *U2AF35*-transduced cells, showed reduced cell proliferation (Fig. 5b and Supplementary Fig. 15b) with a marked increase in the G2/M fraction (G2/M arrest) together with enhanced apoptosis as

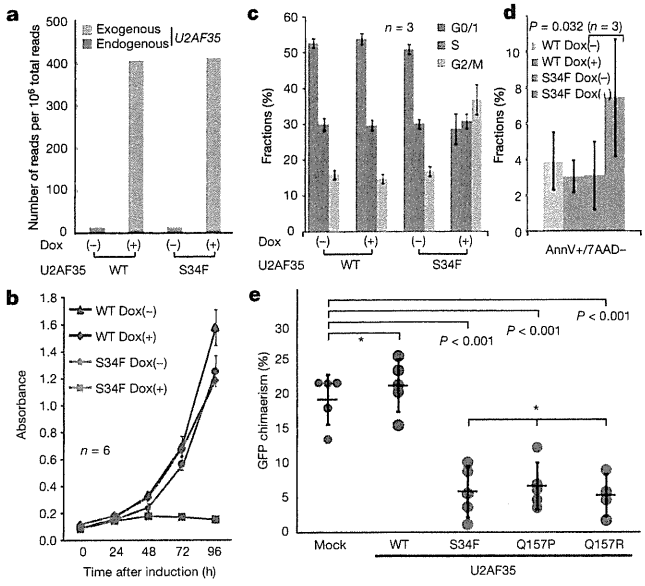

Figure 5 | Functional analysis of mutant U2AF35. a, Expression of endogenous and exogenous *U2AF35* transcripts in HeLa cells before and after induction determined by RNA sequencing. *U2AF35* transcripts were differentially enumerated for endogenous and exogenous species, which were discriminated by the Flag sequence. **b**, Cell proliferation assays of *U2AF35*-transduced HeLa cells, where cell numbers were measured using cell-counting apparatus and are plotted as mean absorbance ± s.d. **c**, The flow cytometry analysis of propidium iodide (PI)-stained HeLa cells transduced with the different U2AF35 constructs. Mean fractions ± s.d. in G0/G1, S and G2/M populations after the induction of U2AF35 expression are plotted. **d**, Fractions of the annexin V-positive (AnnV+) populations among the 7-amino-actinomycin D (7AAD)-negative population before and after the induction of U2AF35 expression are plotted as mean ± s.d. for indicated samples. The significance of difference was determined by paired *t*-test. **e**, Competitive reconstitution assays for CD34-negative KSL cells transduced with indicated U2AF35 mutants. Chimaerism in the peripheral blood 6 weeks after transplantation are plotted as mean %EGFP-positive Ly5.1 cells ± s.d., where outliers were excluded from the analysis. The significance of differences was evaluated by the Grubbs test with Bonferroni's correction for multiple testing. *not significant.

indicated by the increased sub-G1 fraction and annexin V-positive cells (Fig. 5c, d, Supplementary Fig. 14b and Supplementary Methods VI). To confirm the growth-suppressive effect of U2AF35 mutants *in vitro*, a highly purified haematopoietic stem cell population ($CD34^-$c-$Kit^+Scal^+Lin^-$, $CD34^-$KSL) prepared from C57BL/6 (B6)-Ly5.1 mouse bone marrow[28] was retrovirally transduced with either the mutant (S34F, Q157P and Q157R) or wild-type *U2AF35*, or the mock constructs, each harbouring the EGFP marker gene (Supplementary Fig. 16). The ability of these transduced cells to reconstitute the haematopoietic system was tested in a competitive reconstitution assay. The transduced cells were mixed with whole bone marrow cells from B6-Ly5.1/5.2 F1 mice, transplanted into lethally irradiated B6-Ly5.2 recipients, and peripheral blood chimaerism derived from EGFP-positive cells was assessed 6 weeks after transplantation by flow cytometry. We confirmed that each recipient mouse received comparable numbers of EGFP-positive cells among the different retrovirus groups by estimating the percentage of EGFP-positive cells and overall proliferation in transduced cells by *ex vivo* tracking. Also no significant difference was observed in their homing capacity to bone marrow as assessed by transwell migration assays (Supplementary Fig. 17). As shown in Fig. 5e, the wild-type *U2AF35*-transduced cells showed a slightly higher reconstitution capacity than the mock-transduced cells. On the other hand, the recipients of the cells transduced with the various *U2AF35* mutants showed significantly lower EGFP-positive cell chimaerism than those of either the mock- or the wild-type *U2AF35*-transduced cells, indicating a compromised reconstitution capacity of the haematopoietic stem/progenitor cells expressing the U2AF35 mutants. In summary, these mutants lead to loss-of-function of U2AF35 most probably by acting in a dominant-negative fashion to the wild-type protein.

Discussion

Our whole-exome sequencing study unexpectedly unmasked a complexity of novel pathway mutations found in approximately 45% to 85% of myelodysplasia patients depending on the disease subtypes, which affected multiple but distinctive components of the splicing machinery and, as such, demonstrated the unquestionable power of massively parallel sequencing technologies in cancer research.

The RNA splicing system comprises essential cellular machinery, through which eukaryotes can achieve successful transcription and guarantee the functional diversity of their protein species using alternative splicing in the face of a limited number of genes[29]. Accordingly, the meticulous regulation of this machinery should be indispensable for the maintenance of cellular homeostasis[30], deregulation of which causes severe developmental abnormalities[31,32]. The current discovery of frequent mutations of the splicing pathway in myelodysplasia, therefore, represents another remarkable example that illustrates how cancer develops by targeting critical cellular functions. It also provides an intriguing insight into the mechanism of 'cancer specific' alternative splicing, which have long been implicated in the development of cancer, including MDS and other haematopoietic neoplasms[33,34].

In myelodysplasia, the major targets of spliceosome mutations seemed to be largely confined to the components of the E/A splicing complex, among others to *SF3B1*, *SRSF2*, *U2AF35* and *ZRSR2*, and to a lesser extent, to *SF3A1*, *SF1*, *U2AF65* and *PRPF40B*. The broad coverage of the wide spectrum of spliceosome components in our exome sequencing was likely to preclude frequent involvement of other components on this pathway (Supplementary Fig. 18). The surprising frequency and specificity of these mutations in this complex, together with the mutually exclusive manner they occurred, unequivocally indicate that the compromised function of the E/A complex is a hallmark of this unique category of myeloid neoplasms, playing a central role in the pathogenesis of myelodysplasia. The close relationship between the mutation types and unique disease subtypes also support their pivotal roles in MDS.

Given the critical functions of the E/A splicing complex on the precise 3′SS recognition, the logical consequence of these relevant mutations would be the impaired splicing involving diverse RNA species. In fact, when expressed in HeLa cells, the mutant U2AF35 induced global abnormalities of RNA splicing, leading to increased production of transcripts having unspliced intronic sequences. On the other hand, the functional link between the abnormal splicing of RNA species and the phenotype of myelodysplasia is still unclear. Mutant U2AF35 seemed to suppress cell growth/proliferation and induce apoptosis rather than confer a growth advantage or promote clonal selection. *ZRSR2* knockdown in HeLa cells has been reported to also result in reduced viability, arguing for the common consequence of these pathway mutations[35]. These observations suggested that the oncogenic actions of these splicing pathway mutations are distinct from what is expected for classical oncogenes, such as mutated kinases and signal transducers, but could be more related to cell differentiation. Of note in this regard, the commonest clinical presentation of MDS is severe cytopenia in multiple cell lineages due to ineffective haematopoiesis with increased apoptosis rather than unlimited cell proliferation[1]. In this regard, lessons may be learned from the recent findings on the pathogenesis of the 5q− syndrome, where haploinsufficiency of *RPS14* leads to increased apoptosis of erythroid progenitors, but not myeloproliferation[36,37].

A lot of issues remain to be answered, however, to establish the functional link between these splicing pathway mutations and the

pathogenesis of MDS, where the broad spectrum of RNA species affected by impaired splicing hampers identification of responsible gene targets. Moreover, the mutated components of the splicing machinery have distinct function of their own other than direct regulation of RNA splicing, involved in elongation and DNA stability, which may be important to determine specific disease phenotypes. Clearly, more studies are required to answer these questions through understanding of the molecular basis of their oncogenic actions.

METHODS SUMMARY

Whole-exome sequencing of paired tumour/normal DNA samples from the 29 patients was performed after informed consent was obtained. SNP array-based copy number analysis was performed as previously described[17,18]. Mutation analysis of the splicing pathway genes in a set of 582 myeloid neoplasms were performed by first screening mutations in PCR-amplified pooled targets from 12 individuals, followed by validation/identification of the candidate mutations within the corresponding 12 individuals by Sanger sequencing. Flag-tagged cDNAs of the wild-type and mutant *U2AF35* were generated by *in vitro* mutagenesis, constructed into a murine stem cell virus-based retroviral vector as well as a tetracycline-inducible lentivirus-based expression vector, and used for gene transfer to $CD34^-$KSL cells and cultured cell lines, with EGFP marking, respectively. Total RNA was extracted from wild-type or mutant *U2AF35*-transduced HeLa and TF-1 cells, and analysed on microarrays. RNA sequencing was performed according to the manufacturer's instructions (Illumina). Cell proliferation assays (MTT assays) on HeLa and TF-1 cells stably transduced with lentivirus U2AF35 constructs were performed in the presence or absence of doxycycline. For competitive reconstitution assays, $CD34^-$KSL cells collected from C57BL/6 (B6)-Ly5.1 mice were retrovirally transduced with various *U2AF35* constructs with EGFP marking, and transplanted with competitor cells (B6-Ly5.1/5.2 F1 mouse origin) into lethally irradiated B6-Ly5.2 mice 48 h after gene transduction. Frequency of EGFP-positive cells was assessed in peripheral blood by flow cytometry 6 weeks after the transplantation (Supplementary Methods VII). The primer sets used for validation of gene mutations and qPCR of NMD gene expression are listed in Supplementary Tables 9–11. A complete description of the materials and methods is provided in the Supplementary Information. This study was approved by the ethics boards of the University of Tokyo, Munich Leukaemia Laboratory, University Hospital Mannheim, University of Tsukuba, Tokyo Metropolitan Ohtsuka Hospital and Chang Gung Memorial Hospital. Animal experiments were performed with approval of the Animal Experiment Committee of the University of Tokyo.

Received 7 June; accepted 24 August 2011.
Published online 11 September 2011.

1. Corey, S. J. *et al.* Myelodysplastic syndromes: the complexity of stem-cell diseases. *Nature Rev. Cancer* **7,** 118–129 (2007).
2. Ma, X., Does, M., Raza, A. & Mayne, S. T. Myelodysplastic syndromes: incidence and survival in the United States. *Cancer* **109,** 1536–1542 (2007).
3. Bejar, R., Levine, R. & Ebert, B. L. Unraveling the molecular pathophysiology of myelodysplastic syndromes. *J. Clin. Oncol.* **29,** 504–515 (2011).
4. Sanada, M. *et al.* Gain-of-function of mutated *C-CBL* tumour suppressor in myeloid neoplasms. *Nature* **460,** 904–908 (2009).
5. Campbell, P. J. *et al.* Identification of somatically acquired rearrangements in cancer using genome-wide massively parallel paired-end sequencing. *Nature Genet.* **40,** 722–729 (2008).
6. Chapman, M. A. *et al.* Initial genome sequencing and analysis of multiple myeloma. *Nature* **471,** 467–472 (2011).
7. Lee, W. *et al.* The mutation spectrum revealed by paired genome sequences from a lung cancer patient. *Nature* **465,** 473–477 (2010).
8. Ley, T. J. *et al.* DNA sequencing of a cytogenetically normal acute myeloid leukaemia genome. *Nature* **456,** 66–72 (2008).
9. Metzker, M. L. Sequencing technologies — the next generation. *Nature Rev. Genet.* **11,** 31–46 (2010).
10. Shendure, J. & Ji, H. Next-generation DNA sequencing. *Nature Biotechnol.* **26,** 1135–1145 (2008).
11. Shah, S. P. *et al.* Mutational evolution in a lobular breast tumour profiled at single nucleotide resolution. *Nature* **461,** 809–813 (2009).
12. Varela, I. *et al.* Exome sequencing identifies frequent mutation of the SWI/SNF complex gene *PBRM1* in renal carcinoma. *Nature* **469,** 539–542 (2011).
13. Ley, T. J. *et al. DNMT3A* mutations in acute myeloid leukemia. *N. Engl. J. Med.* **363,** 2424–2433 (2010).
14. Mardis, E. R. *et al.* Recurring mutations found by sequencing an acute myeloid leukemia genome. *N. Engl. J. Med.* **361,** 1058–1066 (2009).
15. Yan, X. J. *et al.* Exome sequencing identifies somatic mutations of DNA methyltransferase gene *DNMT3A* in acute monocytic leukemia. *Nature Genet.* **43,** 309–315 (2011).
16. Puente, X. S. *et al.* Whole-genome sequencing identifies recurrent mutations in chronic lymphocytic leukaemia. *Nature* **475,** 101–105 (2011).
17. Nannya, Y. *et al.* A robust algorithm for copy number detection using high-density oligonucleotide single nucleotide polymorphism genotyping arrays. *Cancer Res.* **65,** 6071–6079 (2005).
18. Yamamoto, G. *et al.* Highly sensitive method for genomewide detection of allelic composition in nonpaired, primary tumor specimens by use of Affymetrix single-nucleotide-polymorphism genotyping microarrays. *Am. J. Hum. Genet.* **81,** 114–126 (2007).
19. Wahl, M. C., Will, C. L. & Luhrmann, R. The spliceosome: design principles of a dynamic RNP machine. *Cell* **136,** 701–718 (2009).
20. Tronchère, H., Wang, J. & Fu, X. D. A protein related to splicing factor $U2AF^{35}$ that interacts with $U2AF^{65}$ and SR proteins in splicing of pre-mRNA. *Nature* **388,** 397–400 (1997).
21. Bevilacqua, L. *et al.* A population-specific *HTR2B* stop codon predisposes to severe impulsivity. *Nature* **468,** 1061–1066 (2010).
22. Calvo, S. E. *et al.* High-throughput, pooled sequencing identifies mutations in *NUBPL* and *FOXRED1* in human complex I deficiency. *Nature Genet.* **42,** 851–858 (2010).
23. Haase, D. *et al.* New insights into the prognostic impact of the karyotype in MDS and correlation with subtypes: evidence from a core dataset of 2124 patients. *Blood* **110,** 4385–4395 (2007).
24. Xiao, R. *et al.* Splicing regulator SC35 is essential for genomic stability and cell proliferation during mammalian organogenesis. *Mol. Cell. Biol.* **27,** 5393–5402 (2007).
25. Morin, R. D. *et al.* Somatic mutations altering EZH2 (Tyr641) in follicular and diffuse large B-cell lymphomas of germinal-center origin. *Nature Genet.* **42,** 181–185 (2010).
26. Subramanian, A. *et al.* Gene set enrichment analysis: a knowledge-based approach for interpreting genome-wide expression profiles. *Proc. Natl Acad. Sci. USA* **102,** 15545–15550 (2005).
27. Maquat, L. E. Nonsense-mediated mRNA decay: splicing, translation and mRNP dynamics. *Nature Rev. Mol. Cell Biol.* **5,** 89–99 (2004).
28. Ema, H. *et al.* Adult mouse hematopoietic stem cells: purification and single-cell assays. *Nature Protocols* **1,** 2979–2987 (2007).
29. Chen, M. & Manley, J. L. Mechanisms of alternative splicing regulation: insights from molecular and genomics approaches. *Nature Rev. Mol. Cell Biol.* **10,** 741–754 (2009).
30. Ni, J. Z. *et al.* Ultraconserved elements are associated with homeostatic control of splicing regulators by alternative splicing and nonsense-mediated decay. *Genes Dev.* **21,** 708–718 (2007).
31. He, H. *et al.* Mutations in U4atac snRNA, a component of the minor spliceosome, in the developmental disorder MOPD I. *Science* **332,** 238–240 (2011).
32. Edery, P. *et al.* Association of TALS developmental disorder with defect in minor splicing component *U4atac* snRNA. *Science* **332,** 240–243 (2011).
33. David, C. J. & Manley, J. L. Alternative pre-mRNA splicing regulation in cancer: pathways and programs unhinged. *Genes Dev.* **24,** 2343–2364 (2010).
34. Pajares, M. J. *et al.* Alternative splicing: an emerging topic in molecular and clinical oncology. *Lancet Oncol.* **8,** 349–357 (2007).
35. Shen, H., Zheng, X., Luecke, S. & Green, M. R. The U2AF35-related protein Urp contacts the 3′ splice site to promote U12-type intron splicing and the second step of U2-type intron splicing. *Genes Dev.* **24,** 2389–2394 (2010).
36. Barlow, J. L. *et al.* A p53-dependent mechanism underlies macrocytic anemia in a mouse model of human 5q− syndrome. *Nature Med.* **16,** 59–66 (2010).
37. Ebert, B. L. *et al.* Identification of *RPS14* as a $5q^-$ syndrome gene by RNA interference screen. *Nature* **451,** 335–339 (2008).

Supplementary Information is linked to the online version of the paper at www.nature.com/nature.

Acknowledgements This work was supported by Grant-in-Aids from the Ministry of Health, Labor and Welfare of Japan and from the Ministry of Education, Culture, Sports, Science and Technology, and also by the Japan Society for the Promotion of Science (JSPS) through the 'Funding Program for World-Leading Innovative R&D on Science and Technology (FIRST Program)', initiated by the Council for Science and Technology Policy (CSTP). pGCDNsamIRESEGFP vector was a gift from M. Onodera. We thank Y. Mori, O. Hagiwara, M. Nakamura and N. Mizota for their technical assistance. We are also grateful to K. Ikeuchi and M. Ueda for their continuous encouragement throughout the study.

Author Contributions Y.Sh., Y.Sa., A.S.-O., Y.N., M.N., G.C., R.K. and S.Miyano were committed to bioinformatics analyses of resequencing data. M.Sa., A.S.-O. and Y.Sa. performed microarray experiments and their analyses. R.Y., T.Y., M.O., M.Sa., A.K., M.Sh. and H.N. were involved in the functional analyses of U2AF35 mutants. N.O., M.S.-Y., K.I., H.M., W.-K.H., F.N., D.N., T.H., C.H., S.Miyawaki, S.C., H.P.K. and L.-Y.S. collected specimens and were also involved in planning the project. K.Y., Y.N., Y.Su., A.S.-O. and S.S. processed and analysed genetic materials, library preparation and sequencing. K.Y., M.Sa., Y.Sh., A.S.-O., Y. Sa. and S.O. generated figures and tables. S.O. led the entire project and wrote the manuscript. All authors participated in the discussion and interpretation of the data and the results.

Author Information Sequence data have been deposited in the DDBJ repository under accession number DRA000433. Microarray data have been deposited in the GEO database under accession numbers GSE31174 (for SNP arrays), GSE31171 (for exon arrays) and GSE31172 (for expression arrays). Reprints and permissions information is available at www.nature.com/reprints. The authors declare no competing financial interests. Readers are welcome to comment on the online version of this article at www.nature.com/nature. Correspondence and requests for materials should be addressed to S.O. (sogawa-tky@umin.ac.jp).

THE JOURNAL OF GENE MEDICINE
J Gene Med 2011; **13**: 262–268.
Published online in Wiley Online Library (wileyonlinelibrary.com) **DOI:** 10.1002/jgm.1566

RESEARCH ARTICLE

Minimum requirement of donor cells to reduce the glycolipid storage following bone marrow transplantation in a murine model of Fabry disease

Takayuki Yokoi[1,2*]
Hiroshi Kobayashi[1–3]
Yohta Shimada[1,2]
Yoshikatsu Eto[2]
Nobuyuki Ishige[4]
Teruo Kitagawa[4]
Makoto Otsu[5]
Hiromitsu Nakauchi[5]
Hiroyuki Ida[1–3]
Toya Ohashi[1–3]

[1]*Department of Gene Therapy, Institute of DNA Medicine Higuchi, The Jikei University School of Medicine, Tokyo, Japan*

[2]*Department of Pediatrics, The Jikei University School of Medicine, Tokyo, Japan*

[3]*Institute for Genetic Diseases, The Jikei University School of Medicine, Tokyo, Japan*

[4]*Tokyo Health Service Association, Tokyo, Japan*

[5]*Division of Stem Cell Therapy, Center for Stem Cell and Regenerative Medicine, Institute of Medical Science, University of Tokyo, Tokyo, Japan*

*Correspondence to:
Takayuki Yokoi, The Jikei University School of Medicine, Department of Gene Therapy, Institute of DNA Medicine, Tokyo, Japan
E-mail: t.yokoi@jikei.ac.jp

Received: 7 October 2010
Revised: 14 April 2011
Accepted: 19 April 2011

Abstract

Background Fabry disease (FD) is a lysosomal storage disorders characterized by a deficiency of the lysosomal enzyme, α-galactosidase A. This results in the accumulation of glycolipids, mainly globotriaosylceramide (GL-3), in the lysosomes of various organs. Although bone marrow transplantation and hematopoietic stem cell-based gene therapy can offer the potential of a curative therapeutic outcome for FD, the minimum requirement of donor cells or gene-corrected cells to reduce GL-3 levels is not known.

Methods Lethally-irradiated FD mice were transplanted intravenously with normal bone marrow cells (Ly5.1 positive) mixed with those of FD mice (Ly5.2 positive) at various ratios to investigate the level of engraftment and enzyme activity necessary to effect a reduction in GL-3 storage.

Results Chimerism of whole white blood cells of recipients' peripheral blood remained stable at 8 weeks after transplantation, and chimerism of granulocytes, monocytes, B cells and T cells was equal to that of white blood cells. GL-3 levels were significantly reduced in the lung and heart of animals with a 30% and 50% chimera, respectively. The extent of reduction in these mice was almost identical to that with 100% chimera.

Conclusions In FD mice, reconstitution with 100% donor cells is not required to obtain a therapeutic effect following bone marrow transplantation. These results suggest that a 30% gene correction might be sufficient to reverse disease manifestations in FD. Copyright © 2011 John Wiley & Sons, Ltd.

Keywords bone marrow transplantation; cell-targeted gene therapy; chimerism; Fabry disease; hematopoietic stem

Introduction

Fabry disease (FD; OMIM 301 500), an X-linked lysosomal storage disorder (LSD), results from a deficiency of α-galactosidase A (α-Gal A) and the consequent accumulation of the principal substrate, globotriaosylceramide (GL-3) in various tissues, including the vascular endothelium, renal glomeruli and tubules, dorsal root ganglia, cardiac myocytes and valves, digestive organs and valves, cornea and skin. Clinical features include angiokeratoma, acroparaesthesia, proteinuria, progressive renal impairment, cardiac hypertrophy, gastrointestinal symptoms, corneal opacities, hypohidrosis and impaired temperature regulation. Although FD is an X-linked disease, some heterozygous females present with severe

symptoms because of random X chromosome inactivation [1]. The estimated incidence of FD is one per 40 0000–117 000 live male births [2], although recent studies suggest that the incidence may be higher [3,4].

Enzyme replacement therapy (ERT) is now available for FD [5,6]. This therapy is effective to a certain extent, although patients have to undergo repeated infusions every 2 weeks for their whole lives. Moreover, the induction of an antibody response against the infused recombinant-enzyme can be problematic [7–10]. Although bone marrow transplantation (BMT) can provide an effective and potentially curative therapy for LSDs [11], the limited availability of matched donors limits its application. Hematopoietic stem cell (HSC)-targeted gene therapy (GT) can represent an alternative approach for overcoming the shortage of BMT for inborn errors of metabolism. The potential of this therapeutic approach has also been reported in a murine model of FD [12,13]. However, it is very difficult to attain 100% transduction of HSC. Indeed, only 30% of hematopoietic cells were modified in a recent study for HSC-targeted GT for adrenoleukodystrophy [14], another inborn error of metabolism similar to FD. Hence, the minimal requirement of gene-corrected cells to confer therapeutic effect is an obvious concern in HSC-targeted GT for FD.

In BMT, strong conditioning regimens, such as the use of a large dose of chemotherapeutic agent and irradiation, is required for 100% donor cell reconstitution. These harsh conditioning regimens can sometimes cause severe side effects, such as infection and bleeding. Therefore, establishing milder conditioning regimens is very important [15]. If a sufficient therapeutic effect can be realized by a lower number of donor cells, milder conditioning can perhaps be used to minimize the side effects. In this regard, determining the minimal requirement of donor cells necessary to attain a therapeutic effect is important if BMT is to be considered for FD.

Accordingly, in the present study, we generated FD mice with varying number of donor cells and analyzed the levels of α-Gal A and GL-3 in various tissues.

Materials and methods

Animals

FD mice (B6;129-*Gla*^{tm1}Kul/J) [16] were a generous gift from Dr Roscoe O. Brady at the NIH (Bethesda, MD, USA). C57BL/6Ly5.1 mice were purchased from Sankyo Labo Service (Tokyo, Japan). The white blood cells of these mice are distinguishable by Ly5 (CD45) staining; C57BL/6Ly5.1 mice are CD45.1 positive and FD mice are CD45.2 positive. All mice were maintained in our animal facility under standard housing conditions and all experiments were approved by the Institutional Animal Care Committee.

BMT

Bone marrow cells (BMCs) were harvested from femurs and tibias of C57BL/6.Ly5.1 mice and FD mice (8–12 weeks of age). The bone cavity was flushed with phosphate-buffered saline using a 27-G needle and BMCs were filtered through a 70-μm nylon strainer (BD Falcon, Franklin Lakes, NJ, USA). Red blood cells of BMCs were lysed by BD FACS™ Lysing solution (BD Biosciences, San Jose, CA, USA). BMCs from FD mice and C57BL/6.Ly5.1 mice were mixed at various ratios (C57BL/6.Ly5.1 mice cell: 0%, 10%, 30%, 50% and 100%). A total of 1.0×10^7 cells was injected intravenously into lethally irradiated (12 Gy) FD mice (12–14 weeks of age) through a tail vein. Lethal irradiation was performed using the Hitach-MBR1520R irradiator (Hitachi, Tokyo, Japan). The mice were not anesthetized and placed into an acrylic box, although movement was limited to comfortable breathing as a result of the relatively small box size. Delivery of 12 Gy of X-rays was at 20 mA, 150 kV over 5.5 min with a 2.0-mm aluminium filter.

Flow cytometry analysis

Peripheral blood mononuclear cells were collected from treated mice (8 weeks after transplantation) under anesthesia by retro-orbital venous plexus puncture. The red blood cells were lysed using BD FACS™ Lysing solution (BD Biosciences) in accordance with the manufacturer's instructions.

The antibodies and reagents used to determine engraftment levels in different subsets of peripheral blood mononuclear cells were: Ly5.1-FITC, Gr1-PE, Mac1-PE, CD3e-PE, B220-PE (ebioscience, San Diego, CA, USA). Flow cytometry analysis was performed on a FACS Calibur™ (BD Biosciences) and the results analyzed with Cellquest™ Pro (BD Biosciences)

Enzyme activity assay

Enzymatic activity of α-Gal A was assayed using artificial substrates [17]. Briefly, frozen mouse tissue samples were homogenized with a tissue homogenizer NS-310EII (Microtecnichion, Chiba, Japan) for 10 s, twice, in nine volumes of assay buffer (28 mM citric acid/44 mM dibasic sodium phosphate, pH 4.4). The homogenates were centrifuged at 14 000 *g* for 10 min at 4 °C and the resultant supernatants used for analysis. The activity of α-Gal A was measured fluorometrically using the artificial substrate, 4-methylumbelliferyl α-D-galactopyranoside (Sigma-Aldrich, St Louis, MO, USA). Protein concentration was determined by the BCA Protein Assay Kit (Pierce, Rockford, IL, USA) in accordance with the manufacturer's instructions. Activity was expressed as the release of 4-methylumbelliferone (nmol/mg protein/h).

GL-3 analysis

Measurement of GL-3 was carried out using a modification of the method reported by Kitagawa *et al.* [18] using a triple/quadruple Quattro micro tandem mass spectrometer (MS/MS) (Waters, Milford, MA, USA). Briefly, 20 mg of tissue was homogenized in 1 ml of water and the protein concentration of the homogenate assayed using the BCA Protein Assay Kit (Pierce) in accordance with the manufacturer's instructions. Five milliliters of chloroform–methanol (2:1) was added to the homogenate and centrifuged 1,600 g for 5 min at room temperature. The lower phase of the sample was washed once with chloroform:methanol:water (4:48:47). The lower phase of the sample was evaporated by NO at 50 °C and the extracted lipid dissolved in 1 ml of chloroform:methanol (2:1). The GL-3 amount was assayed by MS/MS as described previously.

Statistical analysis

Student's *t*-test was employed for statistically evaluation. $p < 0.05$ was considered statistically significant.

Results

Chimerism in peripheral blood of recipients

To determine the minimum requirement of normal donor cells and α-Gal A activity to reduce the accumulation of glycolipid in FD organs, we transplanted mixtures of BMCs (total 1×10^7) from C57BL/6Ly5.1 ($CD45.1^+$) and the FD mouse ($CD45.2^+$) at various ratios into lethally irradiated FD mice (Table 1). First, we analyzed the chimerism of white blood cells in peripheral blood using fluorescein isothiocyanate (FITC)-labeled anti-CD45.1 antibody at 8 weeks post-transplantation. As expected, the percentage of CD45.1 positive enzyme competent cells in the peripheral blood of transplanted FD mice was almost same as the percentage of CD45.1 positive cells used for the transplant. For example, when we transplanted 50% CD45.1 positive cells and 50% CD45.2 cells to lethally irradiated FD mice, the percentage of CD45.1 cells was approximately 50% (Figure 1A). Next, we analyzed the chimerism of specific lineage cells. We double stained the peripheral blood cells using a FITC-labeled anti-CD45.1 antibody and a phycoerythrin (PE)-labeled antibody against lineage specific markers, such as Mac1 for monocytes, Gr1 for granulocytes, B220 for B cells and CD3 for T cells. The percentage of CD45.1 positive monocytes, granulocytes, T-cells and B-cells was almost the same as the percentage of CD45.1 positive cells used for the transplant (Figure 1B).

Table 1. The chimerism of bone marrow cells for transplantation

Chimerism (%)	=	WT (CD45.1) (%)	+	FD mice (CD45.2) (%)
0		0		100
10		10		90
30		30		70
50		50		50
100		100		0

BM cells harvested from wild-type (WT) (CD45.1) and FD (CD45.2) mice were mixed to chimerism 0%, 10%, 30%, 50% and 100% ($n = 4$ per group). Cells (1×10^7) were transplanted into lethally irradiated (12 Gy) 12-week-old FD mice. BM, bone marrow.

Enzyme activity in each organ

The activity of α-Gal A in various organs was assessed using an artificial substrate (Figure 2). In some organs, a low level of chimerism was sufficient to significantly increase enzyme activity. In the spleen, lung and heart, a 30% chimera increased enzyme activity significantly (Student's *t*-test: $p < 0.05$) compared to tissues from nontreated FD mice. The activities in the spleen, lung and heart of transplanted mice (30% chimerism) corresponded to 41%, 13% and 30% of wild-type levels, respectively. In the liver of mice with a 50% chimera, α-Gal A activity was significantly increased (Student's *t*-test: $p < 0.05$) compared to nontreated FD mice (approximately 8% of wild-type controls). By contrast, even in mice with 100% donor cells, α-Gal A activity in the kidney was not significantly increased compared to nontreated FD mice. This result indicates that the increase in α-Gal A activity in various organs after BMT clearly depends on the number of bone marrow-derived cells in each organ. The heart might be the exception because it did not contain large number of bone marrow derived cells. We speculate that the heart might have taken up a larger amount of the secreted enzyme than the other tissues.

GL-3 levels in each organ

The GL-3 level in each organ was assessed by MS/MS (Figure 3). A 10% chimera in spleen, 30% chimera in liver and 30% chimera in lung significantly reduced GL-3 levels compared to nontransplanted mice (Student's *t*-test: $p < 0.05$). Hearts of mice with a 50% chimera showed significant reductions in GL-3 levels (Student's *t*-test: $p < 0.05$). However, in the kidney, even 100% normal cells did not reduce GL-3 levels. These observations are consistent with the results of enzyme activity measurements. The heart and lung are severely affected in FD. GL-3 reductions in lungs of mice with a 30% chimera and in the hearts of mice with a 50% chimera were similar to mice with a 100% chimera. Because the heart and lung are affected in FD, these results suggest that a 50% of chimera (i.e. because they exhibited an equivalent efficacy to mice

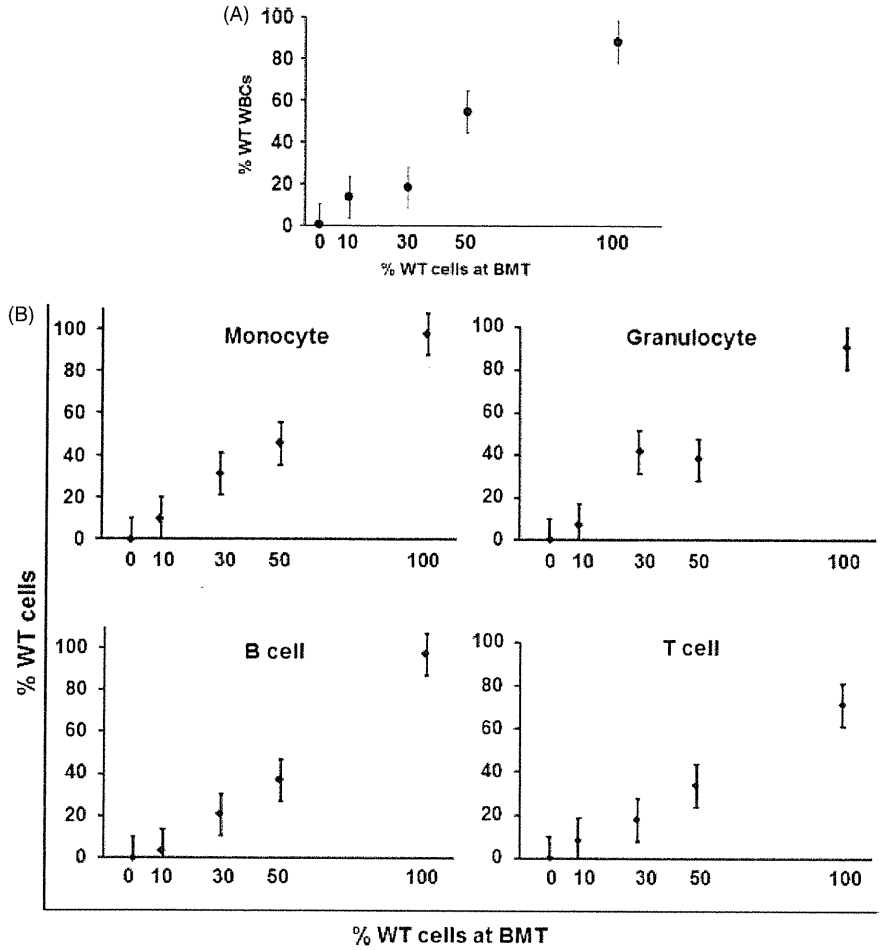

Figure 1. (A) White blood cell (WBC) chimerism in the peripheral blood of a recipient at 8 weeks after transplantation. (B) The distribution of donor cells to T-cells (CD3e), B-cells (B220), monocyte (Mac1) and granulocyte (Gr-1) in the peripheral blood of a recipient at 8 weeks after transplantation. WT, wild-type (indicates C57BL6/LY5.1 mice)

with 100% chimera) may be adequate for BMT of FD. In addition, if HSC-targeted GT is to be considered for FD, at least 50% of HSCs should be transduced.

Discussion

Presently, the only available therapy for FD is ERT. However, neutralizing antibodies against the infused recombinant enzyme developed in some patients that negatively impacted efficacy and caused infusion-related reactions [7–10]. In addition, patients have to receive ERT every 2 weeks for their whole lives. BMT and umbilical cord blood transplantation might overcome the limitations of ERT because we can expect lifelong efficacy once the donor cells are successfully engrafted. Indeed, the efficacy of BMT has been demonstrated in a murine model of FD. However, even with BMT, there are some limitations that have to be overcome. The major limitation of BMT is the limited availability of donors. If we can successfully introduce the normal gene to patients' HSCs, a donor is not required. Clinical trials with HSC-targeted GT have also been performed in other inherited diseases, such as immunodeficiency, and positive outcomes have been reported [19,20]. A HSC-targeted gene therapy trial for Gaucher's disease using retrovirus vector has also been performed [21,22]. However, only few hematopoietic cells were transduced. More recently, clinical trials of HSC-targeted GT for adrenoleukodystrophy were performed using lentivirus vector [12]. In these studies, only 30–40% of the donor hematopoietic cells carried the therapeutic gene. From these studies, we can speculate that HSCs, especially of human origin, are resistant to transduction by viral vectors. It is unclear whether this percentage of donor cells is sufficient to achieve a therapeutic effect. This, for GT approaches for LSDs including FD, the minimal requirement of gene modified cells needs to be clarified.

Studies of chimerism in BMT for other LSDs are being investigated, such as for type 1 Gaucher's disease [23], and mucopolysaccaridosis (MPS) type VII [24]. For example, in type 1 Gaucher's disease mice, it was shown that a 10% chimera is sufficient to improve

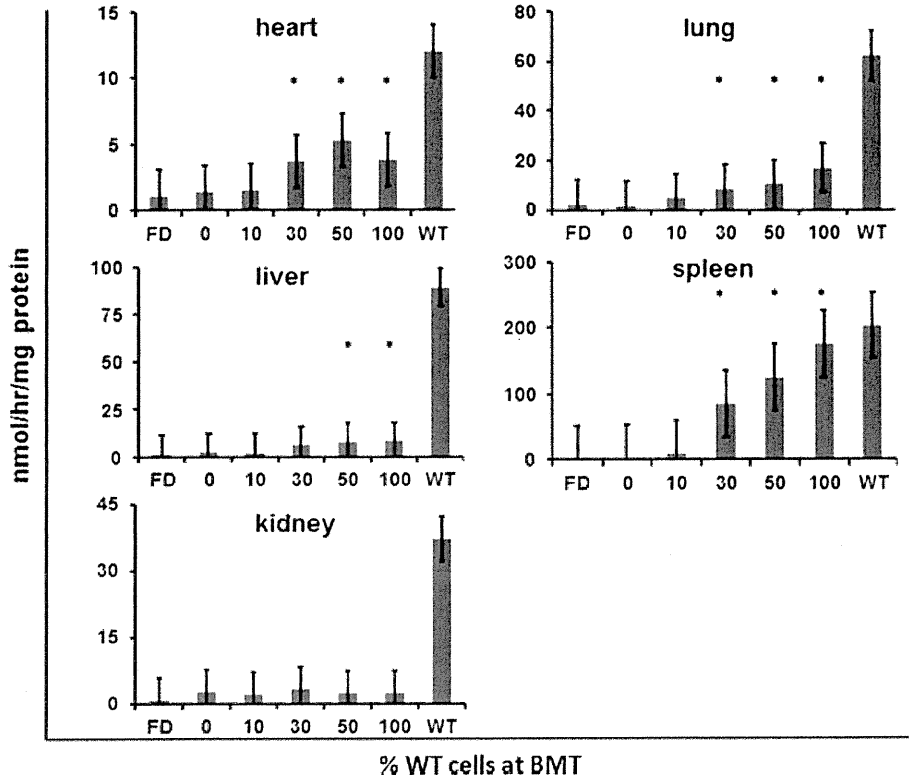

Figure 2. α-Gal A activity in recipient organs ($n = 4$ per group, Student's t-test, $^*p < 0.05$ compared to FD mice) WT, wild-type (indicates C57BL6/LY5.1 mice)

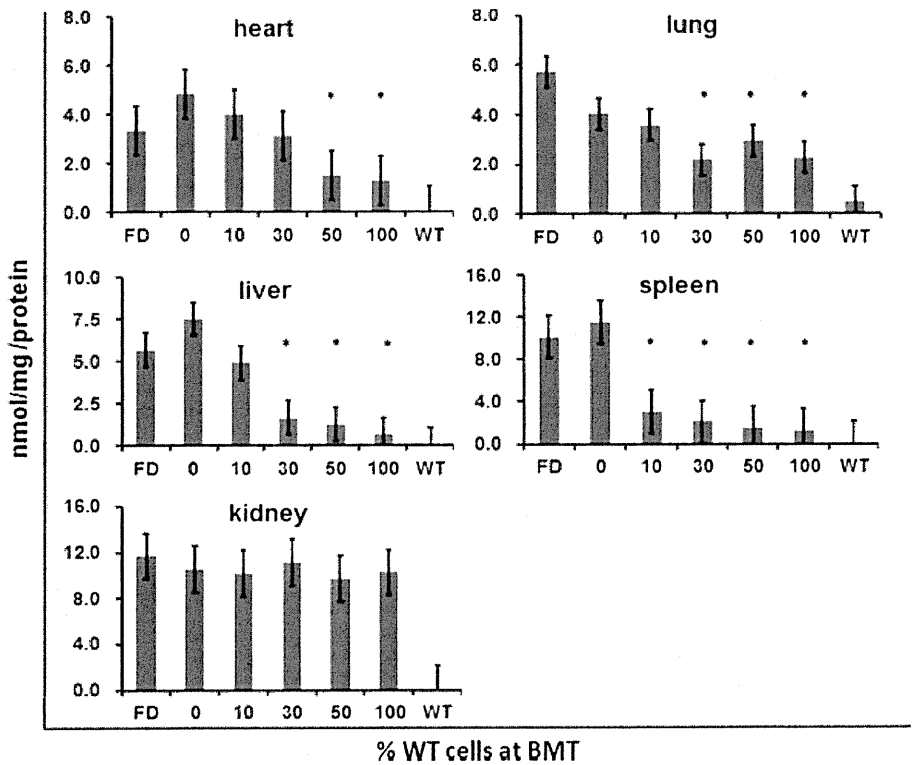

Figure 3. GL-3 storage in recipient organs measured by MS/MS analysis ($n = 4$ per group, Student's t-test, $^*p < 0.05$ compared to FD mice) WT, wild-type (indicates C57BL6/LY5.1 mice)

the pathological findings. In neonatal MPS VII mice, a 10–15% chimera corrected the pathological findings and the malformation of long bones.

In the present study, we assessed the minimum requirement of donor cells necessary to reduce GL-3 levels in the FD mice. As shown by the results obtained, although kidney GL-3 levels remained unchanged even with 100% normal cells, in the heart and lung, which are affected in FD, the low levels of donor cells reduced GL-3 levels in the FD mice compared to nontransplanted mice, and this reduction was similar to that in animals with 100% normal cell engraftment. From these observations, we argue that the transduction of 30–50% HSCs might suffice for maximum efficacy in FD. The kidney is one of the most critical organs for FD, although the heart is as critical as the kidney and there are patients who only develop cardiac involvement (e.g. so-called cardiac variants) [25]. In addition, recent reports including our own, showed that a high percentage of female FD patients develop cardiac involvement [1,26]. Accordingly, such patients are good candidates for HSC-targeted gene therapy and BMT. Because it is difficult to treat renal disease of FD by cell therapy, some patients who received BMT also might continue ERT to prevent the progression of renal symptoms. However, the formation of antibody to the recombinant enzyme might occur. There are reports that antibody formation to recombinant-enzyme did not occur in MPS VI patient after BMT [27]. Rather, the combination therapy (i.e. ERT and BMT) might be more effective than BMT alone [28–30]. There are reports that gene therapy can reduce the risk of antibody formation to administration of recombinant enzyme in Pompe mice [31,32] and immunomodulatory GT also may prevent antibody formation and lethal hypersensitivity [33].

Our observations in the present study provide very useful information not only for HSC-targeted gene therapy, but also for BMT. The main concerns of BMT are the high morbidity and mortality caused by the need for strong preconditioning regimes. Unlike cancer or immune-deficient diseases, the immune function of FD is normal, so that extensive conditioning including high-dose chemotherapy and irradiation are required to achieve 100% engraftment. Nevertheless, these strong pre-conditioning regimens might cause infection and bleeding in recipients. The results obtained in the present study clearly indicate that 30–50% engraftment is sufficient. Thus, we can employ weaker preconditioning regimens to avoid high mortality and morbidity.

In summary, we have shown that a low level of chimerism of normal cells is sufficient to reduce the accumulation of substrates in FD. Furthermore, stem cell therapy or stem cell-based GT might require only a low level of normal or gene-corrected cells for a beneficial therapeutic outcome. These results indicate the possibility of developing effective and efficient protocols for treating FD.

Acknowledgements

The authors wish to thank Ms Sayoko Iizuka and Ms Eiko Kaneshiro for their excellent technical assistance. We also thank Dr R. O. Brady at NIH for kindly providing the FD mouse model mice and Seng H. Cheng for critically reading the manuscript. This study was supported by a grant for the Research on Measures for Intractable Disease, from the Japanese Ministry of Health, Labour and Welfare. Y.E, H.I and T.O have received grant support from Genzyme Corporation, which is a manufacturer of enzymes for FD. H.K, Y.E, H.I and T.O are members of the Department of Genetic Diseases & Genome Science, The Jikei University School of Medicine, which has received grants from Genzyme Corporation. These activities have been fully disclosed and are managed under a Memorandum of Understanding with the conflict of Interest Resolution Board of the Jikei University School of Medicine.

References

1. Kobayashi M, Ohashi T, Sakuma M, Ida H, Eto Y. Clinical manifestations and natural history of Japanese heterozygous females with Fabry disease. *J Inherit Metab Dis* 2008; DOI: 10.1007/s10545-007-0740-6.
2. Desnick RJ, Ioannou YA, Eng CM. Alpha-galactosidase a deficiency: Fabry disease. In *The Metabolic and Molecular Bases of Inherited Disease* (8th edn), Scriver CR, Beaudetal, Sly WS, Valle D, eds. McGraw-Hill: New York, NY, 2001; 3733–3774.
3. La Marca G, Casetta B, Malvagia S, Guerrini R, Zammarchi E. New strategy for the screening of lysosomal storage disorders: the use of the online trapping-and-cleanup liquid chromatography/mass spectrometry. *Anal Chem* 2009; **81:** 6113–6121.
4. Spada M, Pagliardini S, Yasuda M, *et al.* High incidence of later-onset fabry disease revealed by newborn screening. *Am J Hum Genet* 2006; **79:** 31–40.
5. Schiffmann R, Murray GJ, Treco D, *et al.* Infusion of alpha-galactosidase A reduces tissue globotriaosylceramide storage in patients with Fabry disease. *Proc Natl Acad Sci USA* 2000; **97:** 365–370.
6. Eng CM, Guffon N, Wilcox WR, *et al.* Safety and efficacy of recombinant human alpha-galactosidase A–replacement therapy in Fabry's disease. *N Engl J Med* 2001; **345:** 9–16.
7. Ohashi T, Iizuka S, Ida H, Eto Y. Reduced alpha-Gal A enzyme activity in Fabry fibroblast cells and Fabry mice tissues induced by serum from antibody positive patients with Fabry disease. *Mol Genet Metab* 2008; **94:** 313–318.
8. Ohashi T, Sakuma M, Kitagawa T, Suzuki K, Ishige N, Eto Y. Influence of antibody formation on reduction of globotriaosylceramide (GL-3) in urine from Fabry patients during agalsidase beta therapy. *Mol Genet Metab* 2007; **92:** 271–273.
9. Linthorst GE, Hollak CE, Donker-Koopman WE, Strijland A, Aerts JM. Enzyme therapy for Fabry disease: neutralizing antibodies toward agalsidase alpha and beta. *Kidney Int* 2004; **66:** 1589–1595.
10. Schiffmann R, Ries M, Timmons M, Flaherty JT, Brady RO. Long-term therapy with agalsidase alfa for Fabry disease: safety and effects on renal function in a home infusion setting. *Nephrol Dial Transplant* 2006; **21:** 345–354.
11. Krivit W, Aubourg P, Shapiro E. Bone marrow transplantation as effective

treatment of central nervous system disease in globoid cell leukodystrophy, metachromatic leukodystrophy, adrenoleukodystrophy, mannosidosis, fucosidosis, aspartylglucosaminuria, Hurler, Maroteaux-Lamy, and Sly syndromes, and Gaucher disease type III. *Curr Opin Neurol* 1999; **12:** 167–176.

12. Ohshima T, Schiffmann R, Murray GJ, *et al.* Aging accentuates and bone marrow transplantation ameliorates metabolic defects in Fabry disease mice. *Proc Natl Acad Sci USA* 1999; **96:** 6423–6427
13. Takenaka T, Murray GJ, Qin G, *et al.* Long-term enzyme correction and lipid reduction in multiple organs of primary and secondary transplanted Fabry mice receiving transduced bone marrow cells. *Proc Natl Acad Sci USA* 2000; **97:** 7515–7520.
14. Cartier N, Hacein-Bey-Abina S, Bartholomae CC, *et al.* Hematopoietic stem cell gene therapy with a lentiviral vector in X-linked adrenoleukodystrophy. *Science* 2009; **326:** 818–823.
15. Liang SB, Yoshimitsu M, Poeppl A, *et al.* Multiple reduced-intensity conditioning regimens facilitate correction of Fabry mice after transplantation of transduced cells. *Mol Ther* 2007; **15:** 618–627.
16. Ohshima T, Gary J. Murray, William D. Swaim, *et al.* α-Galactosidase A deficient mice: a model of Fabry disease. *Proc Natl Acad Sci USA* 1997; **94:** 2540–2544.
17. Takenaka T, Qin G, Brady RO, Medin JA. Circulating alpha-galactosidase A derived from transduced bone marrow cells: relevance for corrective gene transfer for Fabry disease. *Hum Gene Ther* 1999; **10:** 1931–1939.
18. Kitagawa T, Ishige N, Suzuki K, *et al.* Non-invasive screening method for Fabry disease by measuring globotriaosylceramide in whole urine samples using tandem mass spectrometry. *Mol Genet Metab* 2005; **85:** 196–202.
19. Aiuti A, Cattaneo F, Galimberti S, *et al.* Gene therapy for immunodeficiency due to adenosine deaminase deficiency. *N Engl J Med* 2009; **360:** 447–458.
20. Boztug K, Schmidt M, Schwarzer A, *et al.* Stem-cell gene therapy for the Wiskott–Aldrich syndrome. *N Engl J Med* 2010; **363:** 1918–1927.
21. Dunbar CE, Kohn DB, Schiffmann R, *et al.* Retroviral transfer of the glucocerebrosidase gene into CD34+ cells from patients with Gaucher disease: in vivo detection of transduced cells without myeloablation. *Hum Gene Ther* 1998; **9:** 2629–2640.
22. Dunbar C, Kohn D. Retroviral mediated transfer of the cDNA for human glucocerebrosidase into hematopoietic stem cells of patients with Gaucher disease. A phase I study. *Hum Gene Ther* 1996; **7:** 231–253.
23. Enquist IB, Nilsson E, Månsson JE, Ehinger M, Richter J, Karlsson S. Successful low-risk hematopoietic cell therapy in a mouse model of type 1 Gaucher disease. *Stem Cells* 2009; **27:** 744–752.
24. Soper BW, Lessard MD, Vogler CA, *et al.* Nonablative neonatal marrow transplantation attenuates functional and physical defects of beta-glucuronidase deficiency. *Blood* 2001; **97:** 1498–1504.
25. Nakao S, Takenaka T, Maeda M, *et al.* An atypical variant of Fabry's disease in men with left ventricular hypertrophy. *N Engl J Med* 1995; **333:** 288–293.
26. Mehta A, Clarke JT, Giugliani R, *et al.* Natural course of Fabry disease: changing pattern of causes of death in FOS – Fabry outcome. *J Med Genet* 2009; **46:** 548–552.
27. Whitley CB, Utz JR. Maroteaux–Lamy syndrome (mucopolysaccharidosis type VI): a single dose of galsulfase further reduces urine glycosaminoglycans after hematopoietic stem cell transplantation. *Mol Genet Metab.* 2010; **101:** 346–348.
28. Tolar J, Grewal SS, Bjoraker KJ, *et al.* Combination of enzyme replacement and hematopoietic stem cell transplantation as therapy for Hurler syndrome. *Bone Marrow Transplant* 2008; **41:** 531–535.
29. Cox-Brinkman J, Boelens JJ, Wraith JE, *et al.* Haematopoietic cell transplantation (HCT) in combination with enzyme replacement therapy (ERT) in patients with Hurler syndrome. *Bone Marrow Transplant* 2006; **38:** 17–21.
30. Grewal SS, Wynn R, Abdenur JE, *et al.* Safety and efficacy of enzyme replacement therapy in combination with hematopoietic stem cell transplantation in Hurler syndrome. *Genet Med* 2005; **7:** 143–146.
31. Douillard-Guilloux G, Richard E, Batista L. Partial phenotypic correction and immune tolerance induction to enzyme replacement therapy after hematopoietic stem cell gene transfer of alpha-glucosidase in Pompe disease. *J Gene Med* 2009; **11:** 279–287.
32. Kyosen SO, Iizuka S, Kobayashi H, *et al.* Neonatal gene transfer using lentiviral vector for murine Pompe disease: long-term expression and glycogen reduction. *Gene Ther* 2010; **17:** 521–530.
33. Sun B, Kulis MD, Young SP, *et al.* Immunomodulatory gene therapy prevents antibody formation and lethal hypersensitivity reactions in murine pompe disease. *Mol Ther* 2010; **18:** 353–360.

ELSEVIER

Experimental Hematology

Experimental Hematology 2011;39:351–359

Functional characterization of hematopoietic stem cells in the spleen

Yohei Morita[a,*], Akiko Iseki[a,*], Satoshi Okamura[a], Sachie Suzuki[a], Hiromitsu Nakauchi[a], and Hideo Ema[b]

[a]*Division of Stem Cell Therapy;* [b]*Laboratory of Developmental Stem Cell Biology, Center for Stem Cell Biology and Regenerative Medicine, Institute of Medical Science, University of Tokyo, Tokyo, Japan*

(Received 7 July 2010; revised 13 December 2010; accepted 17 December 2010)

Objective. **Hematopoietic stem cells (HSCs) reside in both bone marrow (BM) and spleen in adult mice. However, whether BM and spleen HSCs are functionally similar is not known. Spleen HSCs were compared with BM HSCs by various assays.**

Materials and Methods. **Whole BM and spleen cells were quantitatively analyzed by competitive repopulation. Single-cell transplantation was performed with HSCs purified from BM and spleen. A parabiosis model was used to distinguish organ-specific HSCs from circulating HSCs. The cell cycle was analyzed with pyronin Y staining and bromodeoxyuridine uptake.**

Results. **Repopulating and self-renewal potentials were similar on a clonal basis between BM and spleen HSCs, whereas the HSC frequency in the spleen was significantly lower than that in the BM. Analysis of parabiotic mice suggested that most HSCs are long-term residents in each organ. Cell-cycle analysis revealed that spleen HSCs cycle twice as frequently as do BM HSCs, suggesting that G_0 phase length is longer in BM HSCs than in spleen HSCs. The cycling difference between BM and spleen HSCs was also observed in mice that had been reconstituted with BM or spleen cells, suggesting that HSC quiescence is regulated in an organ-specific manner.**

Conclusions. **Spleen HSCs and BM HSCs are functionally similar, but their cycling behaviors differ.**

The spleen is a hematopoietic organ in adult mice. During embryonic development, hematopoietic stem cells (HSCs) migrate from the liver and possibly also from the placenta into the spleen around embryonic day 14 as well as into the bone marrow (BM) around embryonic day 17 [1–4]. Thereafter, HSCs reside in both spleen and BM throughout the life of a mouse. The spleen serves as an active hematopoietic organ in lethally irradiated mice for a while after transplantation with BM cells. The spleen is a major site of extramedullary hematopoiesis in pathological conditions, such as myeloproliferative diseases.

Microenvironments or niches are considered to play an important role in the regulation of HSCs [5]. Endosteal and perivascular regions have been proposed for niche sites in the BM [6], and osteoblasts and vascular endothelial cells are considered to be the major components in endosteal and perivascular niches, respectively [7–10]. Other types of cells might be involved in organization of the BM niches [11–14]. Because there are no osteoblasts in the spleen, regulation of HSCs in the spleen may differ from those in the BM. Apart from niches' cellular components, we hypothesized that these two organs contain functionally distinct niches. To gain insight into the niche as a functional entity in stem cell regulation, we compared the functional and behavioral differences between BM and spleen HSCs.

Materials and methods

Mice

C57BL/6 mice congenic for the Ly5 locus (B6-Ly5.1 mice) were bred and maintained at Sankyo Labo Service (Tsukuba, Japan). B6-Ly5.2 mice were purchased from Japan SLC (Hamamatsu, Japan). All procedures were approved by the Animal Care and Use Committee, Institute of Medical Science, University of Tokyo.

*Drs. Morita and Iseki contributed equally to this work.

Offprint requests to: Hideo Ema, M.D., Laboratory of Developmental Stem Cell Biology, Center for Stem Cell and Regenerative Medicine, Institute of Medical Science, University of Tokyo, 4-6-1 Shirokanedai, Minato-ku, Tokyo 108-8639, Japan; E-mail: hema@ims.u-tokyo.ac.jp

Supplementary data associated with this article can be found in the online version at doi:10.1016/j.exphem.2010.12.008.

0301-472X/$ - see front matter.
doi: 10.1016/j.exphem.2010.12.008

Competitive repopulation

Femora, tibiae, and spleen were dissected from 8- to 12-week-old male B6-Ly5.1 mice. Bones were crushed using a mortar and pestle. Spleens were smashed between two glass slides. Cells were suspended in phosphate-buffered saline (PBS). A mixture of 1×10^6 BM or spleen cells (Ly5.1) and 1×10^6 BM cells from B6-Ly5.2 mice was transplanted into each of 10 B6-Ly5.2 mice irradiated at a dose of 9.5 Gy. Peripheral blood cells from the recipient mice were analyzed 4, 8, 12, and 16 weeks after transplantation. After erythrocyte lysis, cells were stained with biotinylated anti-Ly5.1, fluorescein isothiocyanate–conjugated anti-Ly5.2, phycoerythrin-cyanin 7 (PE-Cy7)–conjugated anti-B220, PE-conjugated anti-CD4 and -CD8, and allophycocyanin (APC)-conjugated anti–Mac-1 and –Gr-1 antibodies. The biotinylated antibody was developed with streptavidin-Alexa 594. Cells were analyzed using a FACS Vantage SE flow cytometer equipped with argon (488 nm) and dye (599 nm) lasers (BD Bioscience, San Jose, CA, USA). Percent chimerism was defined as (percent $Ly5.1^+$ test donor cells) (100)/(percent $Ly5.1^+$ test donor cells + percent $Ly5.2^+$ competitor cells). Repopulating unit (RU) values were calculated as (percent chimerism) (number of competitor cells)/(100 − percent chimerism) (10^5) [15].

For in vivo limiting-dilution assays [16], graded numbers of BM or spleen cells from three B6-Ly5.1 mice were mixed with 2×10^5 BM cells from B6-Ly5.2 mice and were transplanted into 10 or more lethally irradiated B6-Ly5.2 mice. When the percentage of chimerism comprising all myeloid, B-lymphoid, and T-lymphoid lineages was 1.0 or more 12 weeks after transplantation, test donor cells were considered to contain one or more multilineage repopulating cells.

HSC purification and transplantation

BM or spleen cells were suspended in PBS. Low-density cells (<1.077 g/mL) were isolated using Ficoll-Paque PLUS (GE Healthcare, Little Chalfont, England). Cells were suspended in 0.05% sodium azide and 3% fetal calf serum in PBS and were stained with a lineage antibody mix consisting of biotinylated anti–Gr-1, -Mac1, -B220, -CD4, -CD8, -Ter119, and –interleukin-7 receptor antibodies (BD Biosciences). Lineage marker–positive cells were depleted using magnetic beads (Miltenyi Biotec, Bergisch Gladbach, Germany). Cells were stained with fluorescein isothiocyanate–conjugated anti-CD34, APC-conjugated anti–c-Kit, PE-conjugated anti–Sca-1, and the lineage antibody-mix antibodies. The biotinylated antibodies were developed with streptavidin–APC-Cy7. Flow cytometric analysis and sorting were performed on a MoFlo flow cytometer equipped with solid (488 nm) and HeNe (633 nm) lasers (Beckman Coulter, Fullerton, CA, USA). Cells were sorted by flow cytometry into screw-cap tubes (Ina Optica, Osaka, Japan) containing 1 mL of 10% fetal calf serum in α–minimal essential medium (Invitrogen, Tokyo, Japan). Cells were mixed with competitor cells at a desired ratio (e.g., 100 $CD34^-KSL$ cells: 2×10^5 competitor cells). For single-cell transplantation, $CD34^-KSL$ cells were individually sorted into each well of a 96-well plate, followed by addition of 2×10^5 competitor cells/well. Cells in 200 μL medium were injected into each of a group of lethally irradiated mice. To perform secondary transplantation, BM cells collected from each femur of all recipient mice were pooled. Each secondary mouse received BM cells equivalent to one-quarter of the total femoral BM of a primary recipient mouse. Peripheral blood cells of the recipient mice were analyzed 12 weeks after transplantation.

Single-cell colony assays

$CD34^-KSL$ cells were sorted into a 96-well plate at one cell per well. Each well contained 200 μL 10% fetal calf serum, 1% bovine serum albumin, 5×10^{-5} M 2β-mercaptoethanol, 10 ng/mL mouse stem cell factor, 10 ng/mL human thrombopoietin, 10 ng/mL mouse interleukin-3, and 2 U/mL human erythropoietin in 200 μL α–minimum essential medium. On day 14 of culture, individual colonies were cytocentrifuged onto glass slides and stained with Hemacolor (Merck, Whitehouse Station, NJ, USA). Cells composing colonies were morphologically classified using light microscopy.

Parabiosis

A B6-Ly5.1 mouse and a B6-Ly5.2 mouse were surgically connected subcutaneously as described [17]. Using pentobarbital anesthesia, two mice underwent unilateral flank skin incisions from elbow to knee joints in mirror image. Mouse-to-mouse skin closure was achieved with an AUTOCLIP Wound Clip Applier using 9-mm clips (BD Biosciences).

Cell-cycle analysis

Lineage-depleted BM cells were suspended in PBS at 1×10^6 cells per milliliter and were incubated with 1 μg/mL pyronin Y (Sigma Aldrich Japan, Tokyo, Japan) at 37°C for 45 minutes. Cells were stained with antibodies as described here, except PE-anti–Sca-1 antibody (replaced by PE-Cy5.5-anti–Sca-1 antibody). Cells were analyzed by FACS Vantage SE or Aria II (BD Biosicences) flow cytometry.

To analyze in vivo cell-cycle kinetics of HSCs, bromodeoxyuridine (BrdU; Sigma-Aldrich Japan) was added to mouse water bottles at 0.5 mg/mL for 3, 7, 14, or 21 days before sacrifice. $CD34^-KSL$ cells purified from BM or spleen were fixed with 70% ethanol at −30°C overnight. After washing, cells were suspended in 25 μL 4M HCl and 0.5% Tween 20 in water at room temperature for 30 minutes. After 300 μL Tris-HCl (pH 8.0) was added, cells were centrifuged. Cells were stained with Alexa 488–conjugated anti-BrdU antibody (Invitrogen) at room temperature for 90 minutes. RNase and propidium iodide were added at 15 μg/mL and 5 μg/mL, respectively. Cells were analyzed by FACSCalibur flow cytometry (BD Biosciences). Alternatively, $CD34^-KSL$ cells were directly sorted by flow cytometry into a droplet on a poly-L-Lys–coated glass slide. Single-cell immunostaining was performed as described [18]. In brief, glass slides were placed in a staining jar containing 100% ethanol for 60 minutes at −30°C. Cells were fixed with 4% paraformaldehyde for 10 minutes and treated with 4N HCl for 10 minutes. Cells were reacted with Alexa 488–conjugated anti-BrdU antibody overnight. After counterstaining with TOTO3 iodide (Invitrogen), cells were analyzed with Arrayscan (Thermo Fisher Scientific, Waltham, MA, USA).

Results

Repopulating activity in spleen cells is lower than that in BM cells

BM or spleen cells (1×10^6 cells) were mixed with BM competitor cells (1×10^6 cells) and the mixture was transplanted into individual lethally irradiated mice. Long-term

multilineage reconstitution was evaluated 16 weeks after transplantation (Fig. 1A and Supplementary Figure E1 [online only, available at www.exphem.org]). As expected, the mean percent chimerism achieved by BM cells was around 50%. However, that achieved by spleen cells was only 6.5%. These data are in good agreement with previous observations that more spleen cells than BM cells are required to reach the same level of repopulation [19]. To evaluate the repopulating activity in a quantitative fashion, the percentage of chimerism was transformed to RU [15]. RU values per 10^6 BM cells or spleen cells were 11.2 or 0.75, respectively. Thus, BM cells had about 15 times as many RU per 10^6 cells as did spleen cells. As shown in Supplementary Figure E1 (online only, available at www.exphem.org), while all myeloid, B-lymphoid, and T-lymphoid lineages were reconstituted by BM cells in every recipient mouse, lymphoid lineages were predominantly reconstituted by spleen cells in four of nine recipient mice. Because we did not observe this sort of lymphoid reconstitution when transplanting whole BM cells, this may have been because only the spleen contained particular B and T lymphocytes capable of surviving for a long time after transplantation. If this is the case, our spleen-cell RU values may be somewhat overestimated.

Frequency of repopulating cells in spleen cells is lower than that in BM cells

In vivo limiting dilution-type analysis was performed to estimate the frequency of repopulating cells in BM or spleen cells. Graded numbers of test donor BM or spleen cells were transplanted in competitive settings. As shown in Figure 1B, the frequency of long-term repopulating cells (LTRCs) in BM was about 1 in 3×10^4 cells, consistent with previous observations [20,21]. On the other hand, that frequency in spleen was about 1 in 3.1×10^5 cells. We examined the frequency of LTRCs in the spleen in another experiment. It was about 1 in 7.3×10^5 cells (data not shown). Thus, the frequency of LTRCs in the spleen was estimated as 1 in 3.1 to 7.3×10^5 cells (on average, $1/5.2 \times 10^5$ cells).

RU, calculated using the percentage of chimerism, represent the amount of repopulating activity in test donor cells [15]. Competitive repopulating units (CRU), determined by limiting dilution assay, represent the number of repopulating cells in test donor cells [16]. The more CRU that are transplanted, the higher the percentages of chimerism or RU obtained. Each CRU has a variety of RU [20], but one can compare the mean RU per single CRU. The mean activity per stem cells (MAS) is defined as (RU per test donor cells) divided by (CRU per test donor cells) [21]. When MAS values are similar for the same numbers of test donor cells from different sources, one can assume that stem cell qualities in these different sources are, on average, similar. BM MAS was 0.34, consistent with previous observations [21]. Spleen MAS was 0.39. Allowing for slight overestimation of spleen RU values, these data suggest that repopulating activity in spleen HSCs, on average, is similar to that in BM HSCs.

Isolation of LTRCs from spleen

CD34-negative/low, c-Kit–positive, Sca-1–positive, lineage marker–negative ($CD34^-KSL$) cells are highly enriched in adult BM HSCs [22]. We asked whether cells with the same markers are similarly enriched in adult spleen HSCs. BM and spleen cells from the same mice were stained with

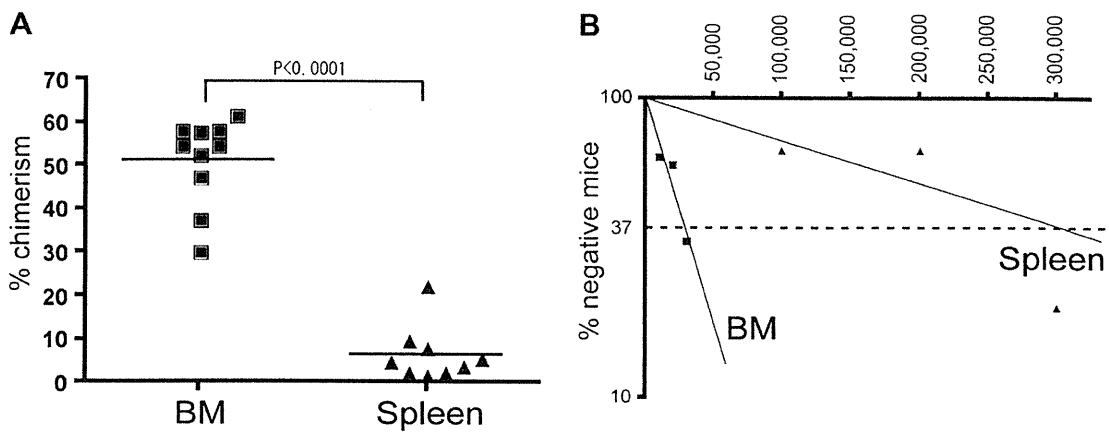

Figure 1. LTRCs in mouse BM or spleen. Two types of competitive repopulating assays were performed on BM and spleen cells from adult mice as described [21,32]. Recipient mice were analyzed 16 weeks after transplantation. (**A**) A mixture of 1×10^6 test donor BM or spleen cells and 1×10^6 BM cells was transplanted into each of 10 lethally irradiated mice. Transplantation of BM cells resulted in 51.3% ± 10.2% percent chimerism (mean ± SD, n = 10). Transplantation of spleen cells resulted in 6.5% ± 6.4% percent chimerism (mean ± SD, n = 9 [one mouse died before analysis]). The percent chimerism conferred by BM cells was significantly greater than that conferred by spleen cells (unpaired *t*-test with Welch correction). See Supplementary Figure E1 (online only, available at www.exphem.org) for myeloid, B-lymphoid, and T-lymphoid lineage reconstitution by BM or spleen cells. (**B**) By limiting dilution assay, the frequency of LTRCs was estimated to be 1 in 29,229 BM cells (95% confidence interval, 1/17,048–1/50,113) or 1 in 307,354 spleen cells (95% confidence interval, 1/158,070–1/597,624).